

DEVELOPMENT OF A METHODOLOGY FOR GEOSPATIAL IMAGE
STREAMING

A THESIS SUBMITTED TO
THE GRADUATE SCHOOL OF NATURAL AND APPLIED SCIENCES
OF
MIDDLE EAST TECHNICAL UNIVERSITY

BY

ERDEM TURKER KIVCI

IN PARTIAL FULFILLMENT OF THE REQUIREMENTS
FOR
THE DEGREE OF MASTER OF SCIENCE
IN
GEODETIC AND GEOGRAPHICAL INFORMATION TECHNOLOGIES

SEPTEMBER 2010

Approval of the thesis:

**DEVELOPMENT OF A METHODOLOGY FOR GEOSPATIAL IMAGE
STREAMING**

submitted by **ERDEM TURKER KIVCI** in partial fulfillment of the requirements
for the degree of **Master of Science in Geodetic and Geographical Information
Technologies Department, Middle East Technical University** by,

Prof. Dr. Canan Özgen
Dean, Graduate School of **Natural and Applied Sciences** _____

Assoc. Prof. Mahmut Onur Karşlıoğlu
Head of Department, **Geodetic and Geographical Inf. Tech.** _____

Assoc. Prof. Dr. Şebnem Düzgün
Supervisor, **Mining Engineering Dept., METU** _____

Examining Committee Members:

Prof. Dr. Vedat Toprak
Geological Engineering Dept., METU _____

Assoc. Prof. Dr. Şebnem Düzgün
Mining Engineering Dept., METU _____

Asst. Prof. Dr. Refik Samet
Computer Engineering, Ankara University _____

Asst. Prof. Dr. Erhan Eren
Information Systems Dept., METU _____

Levent Ucuzal, M.Sc.
General Manager, Bilgi GIS _____

Date: 13.09.2010

I hereby declare that all information in this document has been obtained and presented in accordance with academic rules and ethical conduct. I also declare that, as required by these rules and conduct, I have fully cited and referenced all material and results that are not original to this work.

Name, Last name: ERDEM TURKER KIVCI

Signature : _____

ABSTRACT

DEVELOPMENT OF A METHODOLOGY FOR GEOSPATIAL IMAGE STREAMING

Kıvı, Erdem Türker

M.S., Department of Geodetic and Geographical Information Technologies

Supervisor: Assoc. Prof. Dr. Şebnem Düzgün

September 2010, 109 pages

Serving geospatial data collected from remote sensing methods (satellite images, areal photos, etc.) have become crucial in many geographic information system (GIS) applications such as disaster management, municipality applications, climatology, environmental observations, military applications, etc. Even in today's highly developed information systems, geospatial image data requires huge amount of physical storage spaces and such characteristics of geospatial image data make its usage limited in above mentioned applications. For this reason, web-based GIS applications can benefit from geospatial image streaming through web-based architectures. Progressive transmission of geospatial image and map data on web-based architectures is implemented with the developed image streaming methodology. The software developed allows user interaction in such a way that the users will visualize the images according to their level of detail. In this way geospatial data is served to the users in an efficient way. The main methods used to transmit geospatial images are serving tiled image pyramids and serving wavelet

based compressed bitstreams. Generally, in GIS applications, tiled image pyramids that contain copies of raster datasets at different resolutions are used rather than differences between resolutions. Thus, redundant data is transmitted from GIS server with different resolutions of a region while using tiled image pyramids. Wavelet based methods decreases redundancy. On the other hand methods that use wavelet compressed bitstreams requires to transform the whole dataset before the transmission. A hybrid streaming methodology is developed to decrease the redundancy of tiled image pyramids integrated with wavelets which does not require transforming and encoding whole dataset. Tile parts' coefficients produced with the methodology are encoded with JPEG 2000, which is an efficient technology to compress images at wavelet domain.

Keywords: Image Compression, OGC, WMS, WMTS, Geospatial Raster Data, Wavelet Transformation, Tiled Image Pyramids, JPEG 2000

ÖZ

MEKANSAL İÇERİKLİ GÖRÜNTÜ AKIŞI İÇİN BİR YÖNTEM GELİŞTİRİLMESİ

Kıvcı, Erdem Türker

Yüksek Lisans, Jeodezi ve Coğrafi Bilgi Teknolojileri Bölümü

Tez Yöneticisi: Doç. Dr. Şebnem Düzgün

Eylül 2010, 109 sayfa

Uzaktan algılama yöntemleri (uydular, hava araçları, vb.) ile toplanmış olan mekansal içerikli verilerin sunumu afet yönetimi, belediyecilik, iklim bilimi uygulamaları, çevresel gözlem uygulamaları, askeri uygulamalar gibi birçok alanda önem kazanmıştır. Mekansal içerikli görüntü veri tabanları, günümüz koşullarına göre, fiziksel olarak çok yer kaplamaktadır ve bu verinin sunumu ve iletimi yukarıda sözü edilen alanlarda kullanımını yavaşlatmaktadır. Bu nedenle uygulamaların, mekansal içerikli görüntü sunum hizmetlerini merkezi veri tabanı üzerinden, web tabanlı bir mimari ile sağlamaları gerekmektedir. Mekansal içerikli görüntünün arttırımsal iletimi geliştirilmiş olan görüntü akışı methodunun gerçekleştirilmesi ile sağlanmıştır. Geliştirilmiş olan bu sistem görüntü ile etkileşimleri (görüntü üzerinde gezinme, görüntüye yaklaşma, uzaklaşma vb.) de gözönüne alınarak, kullanıcıların görüntülemek istedikleri veriyi kendileri için anlamlı seviyedeki detayda görüntüleyip kullanmalarına imkan sağlamaktadır. Web üzerinden coğrafi görüntü

iletimi için kullanılmakta olan 2 temel yöntem; bölünmüş görüntü piramitlerinin sunulması ve dalgacık dönüşümü kullanılarak sıkıştırılmış veri bloklarının sunulmasıdır. Coğrafi bilgi sistemlerinde kullanılmakta olan görüntü piramitleri genellikle veri setinin farklı çözünürlükler arasında ki farklarını değil doğrudan kopyalarını içermektedir. Bu nedenle bölünmüş görüntü piramitlerinin aktarılmasında tekrarlı veri aktarımı söz konusudur. Dalgacık dönüşümü tabanlı sıkıştırma yöntemleri ise bütün veri seti üzerinde uygulanması sonrasında kullanıldığından dolayı ancak veri setinin tamamı dönüştürüldükten sonra veri sunulabilmektedir. Geliştirilen görüntü akışı yöntemi ile bölünmüş görüntü piramitlerinin dalgacık dönüşümleriyle bütünleştirilmesiyle tekrar eden veri aktarımı azaltılmış ve veri setinin tamamının dönüştürülmesine gerek kalmadan görüntü iletimi sağlanabilmektedir. Dönüştürülmüş görüntü parçaları dalgacık tabanlı görüntüleri etkin bir biçimde sıkıştırmakta olan JPEG 2000 teknolojisi ile kodlanmıştır.

Anahtar Kelimeler : Görüntü Sıkıştırma, OGC, WMS, WMTS, Coğrafi Rastar Veri, Dalgacık Dönüşümü, Bölünmüş Görüntü Piramidi, JPEG 2000

To my family

ACKNOWLEDGEMENTS

I am very grateful to Assoc. Prof. Dr. Şebnem Düzgün for her guidance suggestions, explanations and encouragement throughout my study. Without her assistance and effort, I could not complete this thesis within the period of M.S. study

Special thanks to my father Çetin and my mother Meral and my sister Yasemin for their endless motivation, understanding and encouragement. I also would like to thank Meral Özkaya for her motivation and support during my study.

I would like to thank to Ministry of Industry & Trade and Bilgi GIS for their financial support to my study (covered in the project “İnternet Tabanlı Mekansal İçerikli Görüntü İletimi Yazılımı”, code of project “00162.STZ.2007-2”) which is funded as a SAN-TEZ project. I also would like to thank to Bilgi GIS family for technical and courage support. Their tolerance and support increased my desire to overcome my thesis.

TABLE OF CONTENTS

ABSTRACT	iv
ÖZ	vi
ACKNOWLEDGEMENTS	ix
TABLE OF CONTENTS	x
LIST OF TABLES	xii
LIST OF FIGURES	xiv
ABBREVIATIONS	xvi
CHAPTERS	
1 INTRODUCTION	1
1.1 REQUIREMENTS TO INCREASE THE PERFORMANCE OF IMAGE TRANSMISSION	2
1.2 METHODS USED TO INCREASE PERFORMANCE OF GEOSPATIAL IMAGE TRANSMISSION	5
1.2.1 TILED IMAGE PYRAMIDS	5
1.2.2 TRANSFORMED AND COMPRESSED IMAGE BITSTREAMS	9
1.3 PROBLEM DEFINITION AND OBJECTIVES	12
2 RASTER DATA MANAGEMENT	16
2.1 CHALLENGES OF RASTER DATA MANAGEMENT	16
2.1.1 SIZE OF GEOSPATIAL IMAGES	16
2.1.2 ARRANGING REQUIRED METADATA	19
2.1.3 OPERATIONS FOR GEOSPATIAL IMAGE TRANSMISSION	20
2.2 RASTER DATA STORAGE	21
3 IMAGE TRANSFORMATIONS	25
3.1 DISCRETE COSINE TRANSFORMATION	25
3.2 KARHUNEN LOEWE TRANSFORMATION	29
3.3 WAVELET TRANSFORMATION	37
4 DEVELOPED METHODOLOGY FOR PROGRESSIVE TILE TRANSMISSION	43
4.1 METHODOLOGY	44
4.2 IMPLEMENTATION	48
4.3 RESULTS AND DISCUSSIONS	52

4.3.1 SCANNED MAPS.....	58
4.3.2 HIGH RESOLUTION ORTHO IMAGES	61
4.3.3 SHADED RELIEFS	63
4.3.4 ALTERNATIVE COMPOSITIONS OF SATELLITE IMAGES	65
4.3.5 BLUE MARBLE NEXT GENERATION.....	68
5 CONCLUSIONS AND RECOMENDATIONS	71
REFERENCES.....	74
ONLINE REFERENCES	76
APPENDICES	
A TEST IMAGE DATASETS.....	77
B SOURCE CODE	88

LIST OF TABLES

TABLES

Table 1.1 Requirements to increase the performance of image transmission.....	2
Table 2.1 Storage Properties of Geographical Raster Datasets For a Region With a Minimum Bounding Box has dimension 50Km x 60km	18
Table 2.2 Comparisson of different raster formats	24
Table 3.1 Eigenvalues related with each components of Landsat TM 7 bands transformation	31
Table 3.2 SNR values of each band for number of components used	32
Table 3.3 RMSE values of each band for number of components used	33
Table 3.4 Eigen Values of single band KLT with row order.....	33
Table 3.5 Eigen Values of single band KLT with resampling order	36
Table 3.6 SNR Values of single band KLT for number of components used	37
Table 3.7 File Sizes of the Wavelet Transformed Lossless Compressed Pyramid Tile Bitsreams With JPEG 2000 and Non-hierarchical PNG Images	42
Table 4.1 Lossy Compressed Image Tile Pyramid hierarchy Size	54
Table 4.2 Comparision of JPEG 2000 encoded Image Tile Pyramid and Progressive Image Tile Pyramid hierarchies SNR	57
Table 4.3 Comparision of JPEG encoded Image Tile Pyramid and Progressive Image Tile Pyramid hierarchies SNR	58
Table 4.4 Lossy compressed DRG-250K-3 image JP2 JPEG and Progressive Tile	

Stream Based on W5x3 SNRs	59
Table 4.5 Lossy compressed Ortho Image-1 image JP2 JPEG and Progressive Tile Stream Based on W5x3 SNRs	62
Table 4.6 Lossy compressed Srtm-relief image JP2 JPEG and Progressive Tile Stream Based on W5x3 SNRs	64
Table 4.7 Lossy compressed Escon-vnir image JP2 JPEG and Progressive Tile Stream Based on W5x3 SNRs	67
Table 4.8 Lossy compressed Bmng-3 image JP2 JPEG and Progressive Tile Stream Based on W5x3 SNRs	69

LIST OF FIGURES

FIGURES

Figure 1.1 A tile image pyramid structure with downsampling factor 2 and 3 resolution levels	6
Figure 1.2 Frequency Components of a Wavelet Transformed Image with 4 resolution levels	10
Figure 1.3 Precincts in a JPEG2000 structure with red dashed lines.....	12
Figure 1.4 General architecture of discussed systems	13
Figure 1.5 Basic model of system that is developed.....	15
Figure 3.1 Flow chart of JPEG progressive coding	28
Figure 3.2 Flow chart of KLT	30
Figure 3.3 Landsat TM Images 7 bands to be transformed with KLT.....	31
Figure 3.4 Landsat TM Images 7 components KLT transformation result.....	32
Figure 3.5 Vector determination function with resampling sample over single band	34
Figure 3.6 Landsat TM Image single component KLT transformation result	35
Figure 3.7 Subband Coding.....	39
Figure 3.8 Wavelet Transformed Landsat TM Image from Izmir region.....	39
Figure 3.9 Single component of Landsat TM Image from Izmir region.....	40
Figure 3.10 Inverse transformation with lifting scheme	40
Figure 3.11 Inverse transformation with lifting scheme	41
Figure 4.1 Flow chart of hybrid methodology developed for progressive image tiles	46
Figure 4.2 Architecture of the Developed Geospatial Image Transmission System.	51
Figure 4.3 Lossless compressed JP2 encoded tiled image pyramids and JP2 encoded Progressive Image Tiles.....	56
Figure 4.4 Number of tiles downloaded with 1Mbps of DRG-250K-3 image with different image pyramid hierarchies	59

Figure 4.5 Number of tiles downloaded with 1Mbps of Ortho-Image-1 image with different image pyramid hierarchies	62
Figure 4.6 Number of tiles downloaded with 1Mbps of Srtm-Relief image with different image pyramid hierarchies	64
Figure 4.7 Number of tiles downloaded with 1Mbps of Escon-vnir image with different image pyramid hierarchies	66
Figure 4.8 Number of tiles downloaded with 1Mbps of Bmng-3 image with different image pyramid hierarchies	69
Figure A.1 Istanbul Landsat Image 1	78
Figure A.2 Istanbul Landsat Image 2	79
Figure A.3 LANDSAT-N36-1 Image	79
Figure A.4 LANDSAT-N36-2 Image	80
Figure A.5 WA State LANDSAT	80
Figure A.6 Escon-vnir Image	81
Figure A.7 WA State Relief	81
Figure A.8 SRTM Relief	82
Figure A.9 Ortho Image 1	82
Figure A.10 Ortho Image 2	83
Figure A.11 Ortho Image 3	83
Figure A.12 Ortho Image 4	84
Figure A.13 Ortho Image 5	84
Figure A.14 Blue Marble Next Generation Image	85
Figure A.15 DRG 250K Image1	86
Figure A.16 DRG 250K Image 2	86
Figure A.17 DRG 250K Image 3	87
Figure A.18 Ancient Piri Reis Map	87

ABBREVIATIONS

GIS	Geographical Information Systems
OGC	Open Geospatial Consortium
WMS	Web Map Service
WMTS	Web Map Tile Service
ECW	Enhanced Compression Wavelet
ECWP	Enhanced Compression Wavelet Protocol
JPEG	Joint Photographic Experts Group
JPIP	JPEG 2000 Interactive Protocol
PNG	Portable Network Graphics
GML	Geography Markup Language
WKT	Well Known Text
WKB	Well Known Binary
BLOB	Binary Large Object
DCT	Discrete Cosine Transformation
KLT	Karhunen Loewe Transformation
DWT	Discrete Wavelet Transformation
SNR	Signal Noise Ratio
RMSE	Root Mean Square Error
STFT	Short time Fourier Transformation
PIT	Progressive image tiles

CHAPTER 1

INTRODUCTION

Geographical Information Systems (GIS) are information systems, which provide to collect, store, query and display data with related spatial information. There are many commercial GIS softwares that are used in the market. However, many of them are desktop applications. GIS starts to take place in nonprofessional people's life in nowadays. The strong development of internet supports to development of GIS as a new architecture, which provides geographical information from sources in different points, covering user requirements at real time (Wu, et al., 2001).

Increasing structure of broadband communication and personal computers that supports high performance distriected graphics, professional data displaying functions became popular with services such as Google Earth, NASA Worldwind and Microsoft Visual Earth (Bettio, et al., 2007). With the emergence of the new generation GIS and geospatial image transmission standards, usage of the web has been one of the most important function of GIS. These popular softwares have many users. In order to construct these softwares effectively, combination of certain technologies have to be used: displaying geospatial images that have high quality at high frame speed as adapted, transmitting spatial data from server to client effectively.

Development of internet, mobile computing technology and wide use of web increases the popularity of GIS on web. Thus, two basic architectures have been developed (Hu , et al., July, 2004): Client-server based web mapping and web

services mapping systems. Web services use agreed common protocols. The most common protocol for geographic data serving is Open GIS Consortiums' (OGC) protocols. These determined standards for web services, by OGC, provide many advantages for using web based GIS. However rendering the results for each query causes low performance which is the significant disadvantage (Hu, 2004). On the other hand, OGC published a new standard web map tile service (WMTS) (Maso, et al., 2010) which will have performance improvements over OGC web map services (WMS) (Beaujardiere, 2004). Furthermore, JPEG 2000 standard part 9 JPEG 2000 Interactive Protocol (JPIP) is one of the most important technologies that are discussed in OGC Community to improve the transmission of spatial data. OGC Web Coverage Service is the center of the interest in discussions in the community to cover the JPIP for spatial data transmission purposes. GIS raster data transmission performance improvement is an active study field which directly affects the commercial products enhancements and increases the frequent usage of GIS.

1.1 REQUIREMENTS TO INCREASE THE PERFORMANCE OF IMAGE TRANSMISSION

Web based GIS generally handles large amount of data and there are several client architecture which uses different types of connections. Due to these facts, visualization and transmission methods and data model used by the system has to be scalable (Komzák , et al., 2003). To provide a scalable system, required capabilities are listed in Table 1.1;

Table 1.1 Requirements to increase the performance of image transmission

ID	Requirement	Type
Req-I	Dataset served has to be randomly accessible.	Data Structure
Req-II	Different scales of dataset have to be accessible.	Data Structure
Req-III	Hierarchical structure of the dataset has to be seamless.	Data Structure

Table 1.1 Continued

ID	Requirement	Type
Req-IV	A good compression ratio has to be provided for efficient transmission of spatial image.	Performance – Network
Req-V	Query and encoding operations must have low computational complexity to serve spatial image to a wide range of clients.	Performance – Complexity
Req-VI	Decoding and reconstruction computational complexity of the server responses must have low computational complexity for different types of client architectures.	Performance – Complexity
Req-VII	Progressive image transmission should be used to decrease redundancy.	Performance – Network
Req-VIII	Developed system should be modular to integrate different features.	Design
Req-IX	Techniques like caching to decrease load on network should applied.	Performance – Network

The first three requirements in Table 1.1 (Req-I, Req-II, Req-III) are directly related with the data structure used. Discussed data structures, tiled image pyramids and wavelet code blocks, provide these requirements. Spatial random access over tiled image pyramids are supplied with query models and indexing methods implemented. Indexing methods declared has low computational complexity which is an essential property for server operations as specified in requirement Req-V. Tile parts used to serve wavelet images (Wu, et al, 2001) and JPEG2000 images structure components; precincts, code blocks, tile part headers (Taubman, et al., 2001) provides spatially random access. Image pyramids and wavelets multi-resolutional structure directly provides access to different scales without resampling from the original.

Req-IV (compression requirement), Req-VII (progressive image transmission requirement) and Req-IX (caching requirement) have to be provided to decrease the load on network and for quick response times. JPIP and ECWP provide direct access over compressed files which have the related file formats. Also client side caching is applicable over systems which use these protocols. Jpeg2000 and ECW file formats used by these protocols provides high compression ratio. A number of compressed code blocks are served in each response with a progressive order. Thus clients could progressively reconstruct the requested image and update the displayed image. On the other hand tiled image pyramids do not support compression natively. However each tile is a separate image so each tile could be compressed with standard image file formats. Generally JPEG format is used to store and transmit each tile. Client side caching is applied for tiles by caching the tiles requested previously (Yang, , et al., 2005) and also caching the tiles that are prefetched (Tu, et al., 2001) for future requests. During prefetching tiles that would probably displayed by the user are requested from the server. By this way if the prefetching is used than the clients have to make requests with information that declares if the request is a prefetching request or user request. Therefore the server could order the request to give high priority to direct user requests. Server would manage request with two different queues. One of the queues would contain prefetch requests and the other one would contain direct user requests. Prefetch queue would be processed only if the direct user request queue is empty.

Low computational complexity of encoding and decoding is a critical issue that severely affects the performance of the system, which was declared in Req-V and Req-VI. Thus the image transformations performance is the key element which is the most important factor encoding process. Integer lifting scheme is preferred in wavelet transformation for fast transformation. Daubechies 9/7 is a good choice for natural image compression (Daubechies, 1992). However Haar transformation is

preferred to because of the kernel length of the filters which affects the number of operations that have to be executed to transform the image (Wu, et al., 2001).

1.2 METHODS USED TO INCREASE PERFORMANCE OF GEOSPATIAL IMAGE TRANSMISSION

There are two main methods to increase performance of transmission of geospatial images; Tiled image pyramids and serving transformed and compressed bitstreams of images. Tiled image pyramids have a well structured hierarchy. Queries over such hierarchy have low computational complexity. However, redundant data is transmitted within different levels of tiles that cover the same region, which causes load over the transmission network. Redundancy could be removed with wavelet transformed compressed code streams. Compressed code blocks are served to clients in order to response user requests. On the other hand transforming and compression GIS datasets that would be provided by the server has to be completed before serving them. Transformation and compression are pre-processes that have to be performed. If the datasource which is used by the server is not a local datasource than whole data set has to be downloaded by the server for pre-processing.

1.2.1 TILED IMAGE PYRAMIDS

Tiling image pyramids and indexing them is a popular way to increase the performance of geospatial image transmission. However, the amount of the data is increased, where the increase ratio depends on resampling factor declared between image pyramid levels. Hierarchical structure of an image tile pyramid is seen in Figure 1.1. Additionally, image pyramids that are used for geospatial images cause redundant data transmission. This redundancy could be decreased with multi-resolution image transformations. The amount of the redundant data without compression could be calculated depending on the amount of the original data (G), the downsampling facto ($dfac$) and the number of levels (lev) used. The extra amount of storage need is calculated nearly 12.5 percent of the original dataset when the downsampling factor is 3 (Tu, et al.,2001). The generalized formula that is used to

calculate the total amount of the storage requirement for a tiled image pyramid is given in Equation 1.1.

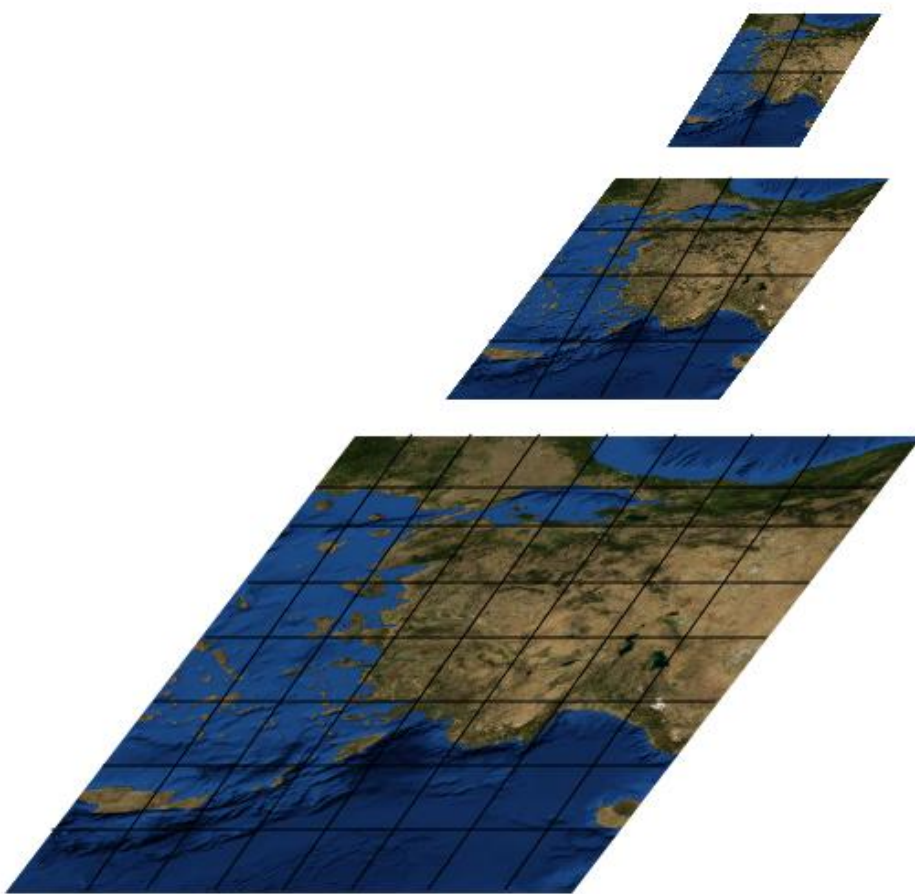


Figure 1.1 A tile image pyramid structure with downsampling factor 2 and 3 resolution levels

$$\sum_{k=0}^{lev-1} \left(\frac{G}{dfrac{2^{2*(lev-k-1)}}} \right) = G * \frac{1 - \frac{1}{dfrac{2^{2*lev}}}}{1 - \frac{1}{dfrac{2^2}}}} \cong \frac{dfrac{2^2}{dfrac{2^2} - 1}} * G \quad 1.1$$

Tiled image pyramids are well organized hierarchical data structure to manage raster datasets. Different scaled regions of resultant sets could be queried over image pyramids. Structure of image pyramids provides development of different query models and indexing mechanisms for multiresolution random access over GIS raster datasets. These queries are executed to reply the basic GIS functions, which are zoom in - zoom out (this requires random access) and pan or go to declared bounding rectangle, which also requires random access. The structure and the query mechanism comes from tile dimensions, which are used in searching methodology over structure, and the number of levels to build pyramid. The main strategy is to find the appropriate resolution level from the client request and find the tiles that have the extent which, intersects with the requested region.

A geometry hierarchy (GH) is defined over an image pyramid which has a downsampling factor 3 (Tu, et al., 2001). The geometry hierarchy is used to access each tile of the pyramid with pan and zoom operations. Each tile is indexed with row and column identifiers related with their current pyramid level. For example, an index over hierarchy $GH(i,j,l)$ maps a tile which is on column i and on row j at level l . The defined hierarchy uses a downsampling factor 3. Hence, 9 neighboring tiles in a square will have the same geospatial extend with the tile at the lower level. The access functions are defined for that state by Tu, et al. (2001). If the resolution of the tiles increases with increasing level than a zoom in n times is declared by Equation 1.2 and zoom out n times is declared in Equation 1.3 for a hierarchy with a downsampling factor d where d is an odd number. Pan operations would be executed over the hierarchy by increasing or decreasing row and column indexes by the related pan direction over the current GH index.

$$\begin{aligned}
& \text{ZoomIn}(GH(i, j, l), n) \\
&= GH \left(d^n * i + \sum_{k=1}^n d^{k-1} * \frac{d-1}{2}, d^n * j \right. \\
&\quad \left. + \sum_{k=1}^n d^{k-1} * \frac{d-1}{2}, l + n \right) \tag{1.2}
\end{aligned}$$

$$\text{ZoomOut}(GH(i, j, l), n) = GH \left(\frac{i}{d^n}, \frac{j}{d^n}, l - n \right) \tag{1.3}$$

Using this indexing method, each tile index required to display the requested region is computed directly by the client. This method is worthwhile for clients that generally requests static scale range between each level. But the new generation GISs clients users scale ranges is not be defined as clear as this state. Since each user type do not need the same pyramid levels of the datasets. Hash indexing function over pyramids (Yang, et al., 2005) method is more applicable in this case. A hash function produces tile identifiers for a bounding box of region of interest. Similar to the previous technique a pyramid contains multi resolutional redundant images of the original dataset. On the other hand geographical coordinates are directly used rather than geometric hierarchy to query over the tiled pyramid structure. Each pyramid level scale and dimension of the geographical extent of a tile (dimX,dimY) and the number of tiles over row R and column C for each level are stored as metadata over the structure. When a client request is made over the structure, the pyramid level which has the most recent scale region requested is identified. Selected region is defined with bounding box where x_1 minimum and x_2 maximum horizontal coordinates, y_1 minimum and y_2 maximum vertical coordinates. The minimum and maximum tile indexes can be calculated by using Equation 1.4 when the dataset coordinates and request uses the same coordinate reference system and the unit vectors that define image coordinates are in the same direction with that reference system.

$$\begin{aligned}
i_1 &= \text{Max}\left(0, \text{Floor}\left(\frac{x_1 - X}{\text{dim}X_{\text{level}}}\right)\right) \\
i_2 &= \text{Min}\left(C_{\text{level}} - 1, \text{Ceil}\left(\frac{x_2 - X}{\text{dim}X_{\text{level}}}\right)\right) \\
j_1 &= \text{Max}\left(0, \text{Floor}\left(\frac{y_1 - Y}{\text{dim}Y_{\text{level}}}\right)\right) \\
j_2 &= \text{Min}\left(R_{\text{level}} - 1, \text{Ceil}\left(\frac{y_2 - Y}{\text{dim}Y_{\text{level}}}\right)\right)
\end{aligned}
\tag{1.4}$$

1.2.2 TRANSFORMED AND COMPRESSED IMAGE BITSTREAMS

Another way to decompose a raster dataset, to provide multiresolutional access and transmission, is transforming images. Image transformations transform images to represent them in a different domain other than the original domain. Image transformations are used for different image processing applications. In this study compression and multi resolutional decomposition are the key capabilities of the image transformations. Most of the image compression formats uses image transformations like cosine transformation and wavelet transformation which decompose an input signal to its frequency components. Generally, lossy image compressions eliminate high frequency components after transformation.

Wavelet transformations is one of the most used transformation method for GIS raster dataset compression. Similar to image pyramid after wavelet transformation raster dataset gains advantage of multiresolutional accessibility. The low frequency component (LL) as seen in Figure 1.2 is the pyramid level which has the lowest resolution. To access to higher resolution inverse wavelet transformation is applied over low frequency and different number of high frequency components HL, LH, and HH as seen in Figure 1.2 according to the requested resolution level. The dimension of the transformed image is the same as the original image. Thus redundancy is not boosted to provide multiresolutional access. On the other hand by signal decomposition the resulting datasets high frequency components entropy is

decreased which causes better compression. Because of these capabilities of wavelet transformation, it is used in different applications and studies in addition to compressed file formats.

LL	HL2	HL1	HLO
LH2	HH2		
LH1		HH1	
LH0			HH0

Figure 1.2 Frequency Components of a Wavelet Transformed Image with 4 resolution levels

Enhanced Compression Wavelet (ECW) is a proprietary image file format developed by Earth Resource Mapping. ECW images could be transmitted progressively. Image data blocks are served to client and compressed blocks are decompressed and the resulting codeblocks are decomposed to build the requested image on client. Only the data blocks requested for the map extents at requested resolution are served to the client. The clients could cache the served data blocks compressed or uncompressed so redundant transmission could be prevented. This provides a significant reduction on network load (Merzhausen, 2001).

The JPEG2000 is a wavelet based image compression standard and it offers many features to support random access to large images. Most important capabilities of JPEG2000 are multi resolutional coding, quality scalability, spatial random access, and highly efficient compression. However, the compression standard itself describes only data structure, suitable to store the compressed data in a file. One way to interact remotely with the image content is to access appropriate blocks from the file as ECWP. Spatial random access is possible, because each code-block is associated with a limited spatial region and is coded independently. This capability is achieved by the precinct structure. The precincts defines collections of spatially adjacent in JPEG2000 image structure (Prandolini, et al., 2003). Precincts divides each resolution level into declared parts for each level seen with dashed red lines in Figure 1.3. JPIP uses precincts in a JPEG2000 file as increments in a progressive image transmission. Precincts dimensions directly affect the performance and behavior of the image transmission process. Smaller dimensions could decrease the update duration but the amount of the metadata is increased to construct the precincts. However, with larger dimensions server responses contains coefficients which are not in the requested regions but near them. On the other hand it is similar to prefetching method for future request. Additionally, wavelet transformation is used without standard image file compression formats for transmission of raster datasets that contains digital elevation data (Kim, et al., 2004) (Bettio, et al., 2007) and geospatial images (Wu, et al., 2001). Wavelet transformation is used to decompose an image to multiresolutional structure with compression (Wu, et al., 2001). Wavelet transformation is applied with next generation wavelet transformations, lifting schemes. Haar transformation is used because of its filters' short length which causes less computation. Client request are replied with compressed wavelet coefficients. When clients get response decompression is applied over the compressed data. After decompression inverse wavelet transformation is applied to reconstruct and display the image. Similar to tiled image pyramids dividing the raster dataset to equal sized blocks is applied. However, this can be applied just over the original level because

multi resolutional structure is achieved by wavelets which are separately applied over each block.

P9	P10	P5 HL	P6 HL	Precinct 1 HL Component	Precinct 2 HL Component
P11	P12	P7 HL	P8 HL		
P5 LH	P6 LH	P5 HH	P6 HH	Precinct 3 HL Component	Precinct 4 HL Component
P7 LH	P8 LH	P7 HH	P8 HH		
Precinct 1 LH Component		Precinct 2 LH Component		Precinct 1 HH Component	Precinct 2 HH Component
Precinct 3 LH Component		Precinct 3 LH Component			

Figure 1.3 Precincts in a JPEG2000 structure with red dashed lines

1.3 PROBLEM DEFINITION AND OBJECTIVES

There are two main methods to increase the performance of geospatial raster transmission over the web; tiled image pyramids and compressing bitstreams of transformed images. A general view of this system can be seen in Figure 1.4. Additionally spatial indexing, client side caching, prefetching are preferred methodologies to increase the performance of transmission of geospatial data. These techniques are developed only for the ordinary local data sources of the GIS servers. On the other hand they are inadequate for the GIS data sources accessed over web with cloud computing approaches. Since in cloud computing approaches, the data sources used by a system will not be managed by the current systems server. Therefore, the pre-processing need to be executed over the whole datasets as seen in Figure 1.4 will not be applicable. However if the dataset content is static or temporal update ranges are known to be metadata than a server side caching will be applicable.

Serving tiles that are originally provided from WMS data sources are server side cached on GeoWebCache server which is an open source project (GeoWebCache is a cache for WMS tiles implemented in Java, 2010). It works like a proxy server between GIS clients and servers. However, it does not deal with the redundancy issue of tiled image pyramids.

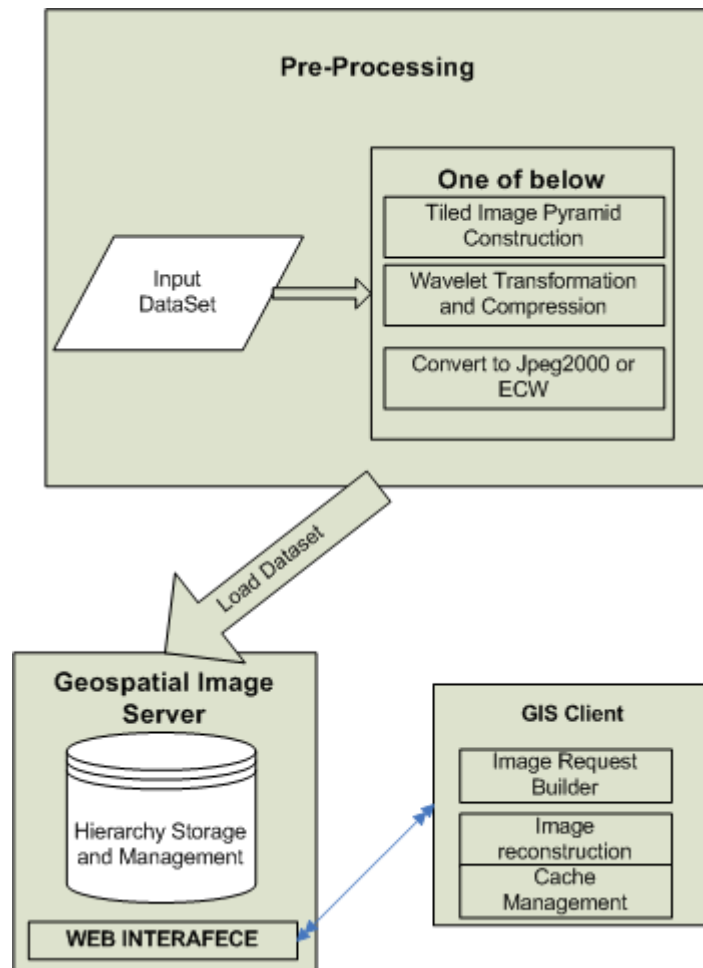


Figure 1.4 General architecture of discussed systems

Tiling image pyramids decreases the response time of queries over the raster datasets. With spatial indexing and caching techniques this method is applicable for the cascaded data sources. On the other hand redundancy over the transmitted data is very high especially when compared to the image transformation techniques.

Compressing transformed bitstream of images provides resolution scalability while decreasing the size of the transmitted images. But these approaches use the image transformation like wavelets and are applied over the full dataset to produce multi resolutional structure of the source dataset. In this case, cascaded data source has to be downloaded to GIS data server in the best resolution. The GIS data server would respond the queries after downloading the whole dataset and transforming it especially for better resolutions of the datasets. Thus, the dataset is not accessible from the GIS server immediately after the registration of the cascaded data source.

In order to overcome above mentioned problems a software system is developed for progressive image transmission. The developed software uses the performance improvement techniques that is applicable over both local and cascaded data sources accessed over the clouds, which has several types of clients; mobile computers to servers. Caching and indexing tiles methodologies is used with the image transformation techniques to improve the performance of the geospatial image transmission. System architecture is like GeoWebCache. Also it has the capability to provide local data sources, prefetching online sources and processing tile groups to perform progressive image transmission. This enables the system to decrease the load on network by decreasing redundancy. A general model which is similar to GeoWebCache is seen in Figure 1.5.

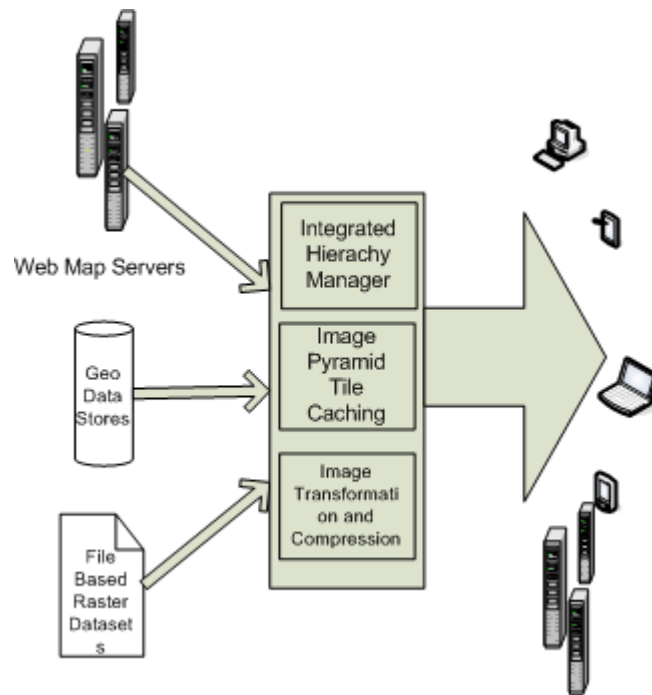


Figure 1.5 Basic model of system that is developed

With this system a tile caching mechanism with wavelet transformations is integrated to decrease the redundancy for efficient use of the bandwidth and data storage. Tiling is used to lower the load on the data source and reduce the computational time for transformation and compression of the response to the client queries. Transformations are planned to decrease the number of queries made by the server over the data source because of their multi-resolutional data representation capabilities. Furthermore transformations frequency decomposition capability over the geospatial image datasets increases the efficiency of entropy coding. The geospatial images (similar to other multimedia) reserves most of the information of the image on lower frequencies and details on higher frequencies.

CHAPTER 2

RASTER DATA MANAGEMENT

Data is the one of the critical element of GIS and beyond spatial data infrastructure (SDI). Data used by GIS is conventionally abstracted by two categories; raster and vector. Geographic features are represented with geometric objects such as points, lines, polygons which are binded to a coordinate reference system(CRS). The datasets that contains a specific type of feature is called vector layer. On the other hand raster layers cover a regions continuous data in GIS. Traditionally raster data used in GIS is abstracted with regular grids that could be referenced with Cartesien coordinate system. In GIS raster layers are referenced to earth by a projection and CRS. The objective of the thesis is related with raster layers so raster data management issues will be discussed in subsequent sections.

2.1 CHALLENGES OF RASTER DATA MANAGEMENT

2.1.1 SIZE OF GEOSPATIAL IMAGES

The objective of the thesis is to develop software that is efficient to transmit geospatial images to the web GIS clients. A GIS server has to manage a region's different raster layers that have different resolution. According to the resolution of the dataset and the regions area the uncompressed size of the layers vary between gigabytes to terabytes.

For example an enterprise's region of interest is limited with a minimum bounding box that has a dimension 50km x 60km on earth. High resolution satellite images with 1 meters spatial resolution, RGB composed and pan-sharpened Landsat images with 15 meter spatial resolution, ortho-rectified aerial images with 30 cm spatial resolution, and scanned maps with scales 1:25000 and 1:100000 are used by the typical enterprise.

Uncompressed sizes of the datasets depend on the number of pixels in the datasets and the number of bytes to represent a pixel. Number of pixels of a dataset with known dimensions on earth could be calculated by using Equation 2.1.

$$pixels = Ceil\left(\frac{regionWidth}{spatialResolution}\right) * Ceil\left(\frac{regionWidth}{spatialResolution}\right) \quad 2.1$$

Scanned map's spatial resolution depends on the two key factors. First the scanner's (which is used for digitization process) technical specification number dots per inch (dpi) and second the source maps scale. Hereby the scanned maps spatial resolution in meters is given in Equation 2.2.

$$spatialResolution = \frac{1}{scale * dpi * 39.3700787} \quad 2.2$$

Let us assume that whole datasets have 3 bands with 8 bits radiometric resolution. With this assumption a pixel is represented with 24 bits, 3 bytes. Let us assume that actual maps are digitized by a scanner which has 600 dpi. Hereby with equations 2.1 and 2.2 datasets raw storage requirements could be calculated as seen in Table 3.1.

Table 2.1 Storage Properties of Geographical Raster Datasets For a Region With a Minimum Bounding Box has dimension 50Km x 60km

Dataset	Spatial Resolution (meters)	Width (Pixel)	Height (Pixel)	Storage Need
High Resolution Satellite Image	1	50000	60000	8.4 GB
Pan-sharpened Landsat Composition	15	3334	4000	38.15MB
Orthophotos	0.3	166667	200000	93 GB
Scanned Map with scale 1:25000 (scanned with 600 dpi)	1.06	47170	56604	7.45GB
Scanned Map with scale 1:100000 (scanned with 600dpi)	4.24	11793	14151	477.43MB
Scanned Map with scale :25000 (scanned with 1200 dpi)	0.53	94340	113208	29.84GB
Scanned Map with scale 1:100000 (scanned with 1200 dpi)	2.12	23585	28302	1.86GB

Calculated storage requirements do not cover storage needs of geographical metadata of raster datasets. However, required metadata to serve geospatial images size is relatively few. Raster datasets' coordinate reference system and geographical projection are required for geospatial image transmission. With the minimum required geographical metadata raster data set could be declared as a GIS layer.

2.1.2 ARRANGING REQUIRED METADATA

GIS servers have to publish the layers' geographical metadata. At the beginning of a geospatial image transmission session GIS client access the metadata of the layers. Clients resolve geographic metadata to build posterior requests over served layers by user interactions. Geographical metadata has to be managed with the raster dataset. The minimum geographical metadata required are spatial reference system, and projection information on that spatial reference system with ground control points or minimum bounding rectangle.

There are different approaches to encode and manage raster datasets' metadata. OGC and ISO/TC211 defined several encoding types to encode the objects that define geographical projection and coordinate reference systems. Also schemas to manage geographical data and related metadata are defined by these organizations.

ISO 19115 defines the schema required for describing geographic information and services (Geographic information - Metadata, 2003). The metadata covered with schema are information about the identification, the extent, the quality, the spatial and temporal schema, spatial reference, and distribution of digital geographic data. ISO 19115 metadata could be encoded and stored with different methods. ISO 19139 defines a XML encoding (Geographic Metadata XML (GMD)) on ISO 19115 metadata (Geographic information -- Metadata -- XML schema implementation, 2007). ISO 19123, which defines a schema to manage coverage data, could be used for raster coverage's that is integrated with the related metadata specifications (Geographic information -- Schema for coverage geometry and functions, 2005).

Geography Markup Language (GML), Well Known Text (WKT) and Well Known Binary (WKB) are the encoding models for geographic features defined by OGC. Spatial Reference Systems can be represented with a textual encoding by WKTs. Spatial reference systems can be represented with a binary encoding with WKBs (Herring, 2006). To manage and access WKTs and WKBs with different

systems (CORBA , OLE/COM, SQL interfaces are defined by OGC. Geographic Markup Language defines objects to cover geographical data and metadata. *gml:AbstractCRS* and *gml:AbstractCoordinateReferenceSystem* are the base object types to define coordinate reference systems. And *gml: RectifiedGrid* object type is defined within Grid Schema to define a grid that could be projected on the declared spatial coordinate system for the grid (Portele, 2007). In addition OGC published GML in JPEG 2000 for Geographic Imagery Encoding Specification to embed gml into JPEG2000 xml boxes. Thus spatial reference system and projection could be encoded within a JPEG2000 file. Additionally specification provides annotating geographic features with the related gml objects on the image.

2.1.3 OPERATIONS FOR GEOSPATIAL IMAGE TRANSMISSION

A GIS stake holder's basic expectations from a map viewing system are to be able to use zoom in, zoom out and pan operations. These operations need random access to geospatial datasets. Moreover for zoom in and zoom out operations resampling of datasets or multi-resolutional access to datasets is required.

Resampling operation has a high complexity. On desktop GIS applications it would be acceptable to wait the resampling for the result a piece of data on the dataset. But the resampling operations complexity would cause high load over o web GIS server. It is trivial that both the responses to the clients that are requested at original or different scale will be delayed because of resampling. Thus web GIS server's needs to access to datasets at different scales. In other words data storage has to provide multi-resolutional access over the geospatial raster dataset.

Other than access operations geospatial operations over datasets could be required for specific use cases. These operations could be listed as; re-projection, rendering vector layers, overlaying different layers, operations on temporal dimension (i.e. change detection), spatial filtering (i.e. low-pass filtering, high-pass filtering,

nonlinear operations), RGB composition from declared layers etc. Performance overhead of these operations over GIS server cannot be solved with data storage methods.

If the processing operations over datasets are predictable for web GIS clients then caching the results of the operations over the datasets on the GIS server could be useful. If the operations on the datasets are designated then, if available, the operation could be executed over the whole related datasets and the results are stored. But if the datasets are updated frequently then these methods individually would be overhead over the GIS server.

2.2 RASTER DATA STORAGE

There are different raster file formats and also database systems to store and manage geospatial images. Some of the image file formats designed to contain metadata and also some of them directly designed for geospatial images, could be used to store and transfer geospatial images. On the other hand standard image file formats that are not designed to contain metadata, geographical or another domains metadata could be used with external metadata to support geospatial images. But in this case there has to be an additional effort to manage and store metadata such as world files. World files which are plain text files contain georeferencing information of the related files. World files have the same name with world file except the "w" character at the end of world file (World files for raster datasets, 2010). For example a JPEG file that contains a part of a high resolution satellite image of Ankara "ankara1.jpeg" would have a world file named "ankara1.jpegw" or "ankara1.jpw" which is located in the same directory with the image file.

There are several file formats related to raster storage, which have different encoding, access and metadata management methodologies.

JPEG JPEG is discrete cosine transform (DCT) and Huffman coding based compressed image file format. JPEG supports lossy and lossless compression. With JPEG compression images could be lossy compressed 1:10 ratio with little or no visual image quality loss. Gray and RGB colored images could be compressed with JPEG. While compressing RGB colored images color space transformation is applied. Images are transformed RGB color space to YUV color space. In YUV color space Y component represents luminance, U and V components represents color information of each pixel. U and V color components are downsampled and their resolution are decreased to half. After color transformation and resampling of components DCT is applied to 8x8 on all three components. After quantizing transformed values with applying Huffman compression process is completed.

GeoTIFF After rectification and reGIStration process geospatial images could be stored in tagged image file format files (TIFF) with geographic reGIStration parameters. GeoTIFF standardize how to store geographic metadata within a TIFF file. Most of the geographic information system software packages supports GeoTIFF. GeoTIFF could contain a JPEG file that is tagged with geographical information. On the other hand GeoTIFF supports lossless compression with methods like LZW and PackBits.

JPEG 2000 JPEG 2000 differentiates from JPEG with wavelet and Embedded Block Coding with Optimal Truncation (EBCOT) techniques. The most important features of JPEG 2000 are high compression ratio lossy and lossless compression, regional compression with region of interest definitions, embedded metadata management with xml boxes, scalable file format support, and different radiometric resolution support, multi-resolutional and spatially random access. JPEG 2000 supports transparency with alpha band. Alpha band is important for geospatial images to represents cells that contains no data values.

ECW Embedded compression wavelet is an open standard that is developed by Earth Resource Mapping Company. Especially for high resolution satellite images and orthophotos efficient compression is achieved with ECW format. Typically ECW file format supports 1:10 to 1:100 compression ratios. Multi-resolutional and spatially random access to ECW files is available. Geographical projection information could be embedded to ECW files. Also with ECW protocol (ECWP) progressive image transmission is supported.

MRSID Multi Resolutional Seamless Image Database (MRSID) is a wavelet based image compression file format. This format is developed from LizardTech Company for GIS. LizardTech's product GeoExpress provides to read and write MRSID images. ExpressView Browser Plug-in supports to view MRSID images via web browsers. The main steps of MRSID image coding could be summarized with; producing multi-resolutional image with wavelet transformation, all resolution levels have 4 subbands coded with 32 bits, all subbands are divided to 64x64 sized blocks, all blocks are divided to sub blocks over bit layers.

The comparison of the formats discussed above can be seen in Table 2.2 which is modified from the technical overview made by ER Mapper at 2002 (Accelerating WebGIS with Image Web Server, 2010).

Database Systems Above methods provides storage by file based systems. There are database systems to manage geospatial images and its metadata. **GeoRaster** is a feature of Oracle spatial. GeoRaster provides to store geospatial images and related metadata. Moreover it provides indexing, query operations, analyzing geospatial images. With Oracle Application Server MapViewer geospatial images could be viewed over map. GeoRaster uses tiled image pyramid structure to provide multi-resolutional and randomly accessible GIS raster datasets. Tile images are stored in blocks that contain Binary Large Objects (BLOB). On the other hand **PostGIS** is another database system to manage geospatial objects like Oracle Spatial. PostGIS is

an extension over open source database management system Posgress. **WKT Raster** is an ongoing project aiming at developing raster support in PostGIS.

Table 2.2 Comparisson of different raster formats

	ECW	MrSID	JPEG 2000	JPEG	GeoTIFF
Coding Base	Wavelet	Wavelet	Wavelet	Discrete Cosine Transform	JPEG, LZW, PackBits, Deflate
Ratio	25:1	25:1	25:1	6:1	2:1
Maximum File Size	Not Limited	2 GB	Not limited	2 GB	2 GB
Maximum width height	32 bit	31bit	32 bit	31 bit	31 bit
Maximum Number Of Bands	2.1 billion	4	Not Limited	3	4
Precision	8 bit , 12 bit	8 bit , 11 bit	1-23 bit	8 bit , 12bit , 16bit	1 bit, 8 bit, 16 bit
Loss-less Compression	No	No	Yes	Yes	Yes
Standard Georeference Metadata	Yes	Yes	With GMLJp2	No	Yes

CHAPTER 3

IMAGE TRANSFORMATIONS

Transform coding is the process to transform an image from a domain to another domain and code image in the transformed domain. Most of the image and video compression formats uses image transformation as the basis of the encoding. Also transformations provide different types of progression other than spatial progression by the exchanged domain.

Transmitting an image that supports progressive access increases the response time of the image request. Image transformations are the key elements of the progressive image transmission. In this chapter Discrete Cosine Transform, Karhunen Loewe Transform and Wavelet Transformations are examined in according to their progressive coding facility.

3.1 DISCRETE COSINE TRANSFORMATION

Discrete Cosine Transform (DCT) is used as the base transformation of JPEG image file format. After dividing images into equally sized blocks each block is transformed with DCT. Thus the transformation coefficients of each block are not affected signal components in neighboring blocks. This causes blocking effect at high compression ratio while using JPEG. After transformation the resulting low frequency components contains the main information of the image. Therefore transformation results would be quantized with a quantization table that would decrease the

coefficients in direct proportion to increase of the frequency. In that case the affect of the high frequency components on the inverse transformed image would be eliminated.

JPEG uses 8x8 sized blocks. Larger block sizes would be more accurate and the blocking effects would be less. But it is faster to compute small blocks. One dimensional DCT on blocks with a width of 8 is seen in Equation 3.1. At transformed domain u is the index of the samples in F , which is the transformed representation of the original function f that is indexed with i . C is constant variable used in transformation (Ze-Nian Li, et al., 2004).

$$F(u) = \frac{1}{2} C(u) \sum_{i=0}^7 \cos\left(\frac{(2i+1)u\pi}{8}\right) * f(i) \quad 3.1$$

Using one dimensional transformation Equation 3.1 2 dimensional transformation equation could be calculated as Equation 3.2.

$$F(u, v) = \frac{1}{4} C(u)C(v) \sum_{i=0}^7 \sum_{j=0}^7 \cos\left(\frac{(2i+1)u\pi}{8}\right) * \cos\left(\frac{(2j+1)v\pi}{8}\right) * f(i, j) \quad 3.2$$

One dimensional inverse discrete cosine transformation (IDCT) on blocks with a width of 8 is seen at Equation 3.3.

$$f(i) = \frac{1}{2} \sum_{u=0}^7 C(u)F(u)\cos\left(\frac{(2i+1)u\pi}{8}\right) \quad 3.3$$

Using one dimensional transformation Equation 3.3 2 dimensional transformation equation could be calculated as Equation 3.4.

$$f(i, j) = \frac{1}{4} \sum_{i=0}^7 \sum_{j=0}^7 C(u)C(v)F(u, v) \cos\left(\frac{(2i + 1)u\pi}{8}\right) * \cos\left(\frac{(2j + 1)v\pi}{8}\right) \quad 3.4$$

In all transformation and inverse transformation equations 3.1, 3.2, 3.3, 3.5 used values C (u) and C (v) are defined as

$$C(u) = \begin{cases} \sqrt{\frac{1}{8}} & \text{for } u = 0 \\ \sqrt{\frac{1}{4}} & \text{otherwise} \end{cases} \quad 3.5$$

DCT transform could be used as a base of a progressive image transmission. For example JPEG uses 2 different file modes to support progressive image transmission, progressive mode and hierarchical mode. Progressive mode manages the order of the transformed and quantized image to support progression. On the other hand hierarchical mode encodes image with an order of increasing resolution to support progression.

JPEG supports progressive coding option with two different methods: Successive Approximation and Spectral Selection. After quantizing the transformed values these coefficients are zig-zag ordered for each block. With spectral selection ordered values are grouped by their index values. Each group is separately entropy coded and streamed from 0 to 63 indexes. With successive approximation each block is binary decomposed and ordered from the most significant bit to least significant bit. The bit

layers are separately entropy coded and streamed from most significant bit layer to least significant bit layer. The flow chart of progressive coding is seen in Figure 3.1. (Yun Q. Shi, et al., 1999)

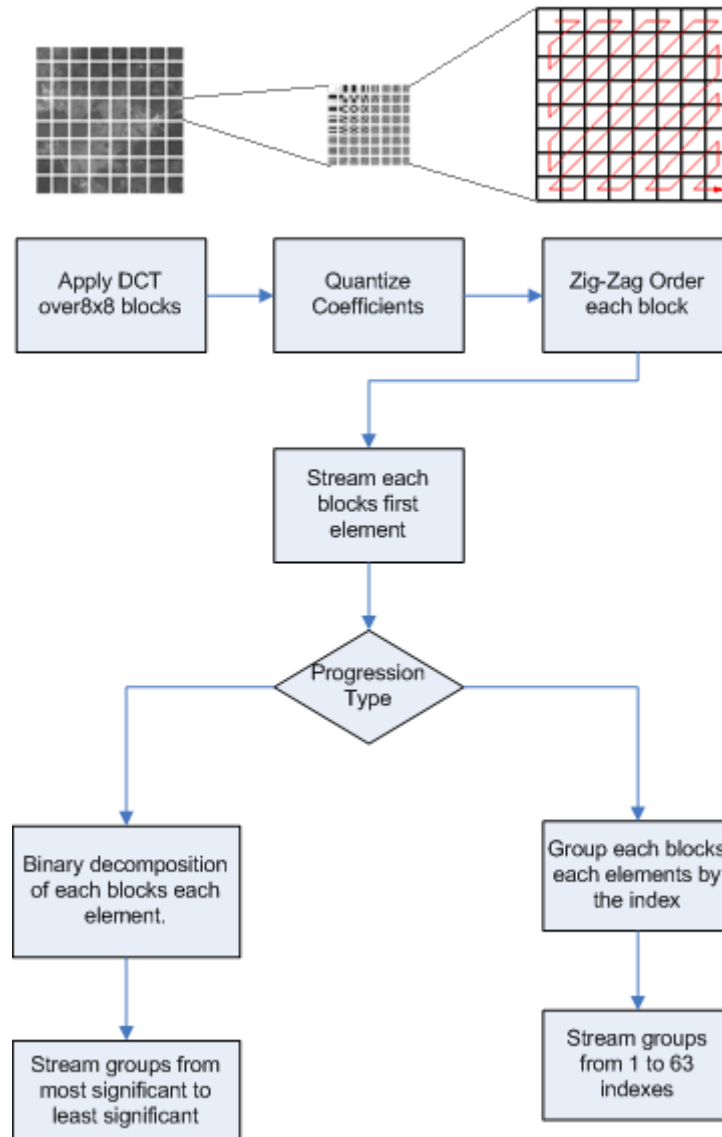


Figure 3.1 Flow chart of JPEG progressive coding

Hierarchical mode uses different resolution levels of an image. First the number of the levels in hierarchy is declared. Image is downsampled by factor of 2 and in number of levels. Encoding is started from the lowest resolution. The encoded image is decoded and upsampled by factor of two. The resulting image is differenced from the image which has the same dimension with the image that is produced in the

downsampling process of the original image. The difference image is encoded. This process is operated for each resolution level similar to differential pulse-code modulation. The lowest resolutions encoded image and the differences are transmitted in order with the related resolution level.

3.2 KARHUNEN LOEWE TRANSFORMATION

In Karhunen Loewe Transformation (KLT) image transformation which is also known as Hotelling Transformation, Principal Component Analysis (PCA) is used in many applications of image processing like face recognition, image compression, and pattern recognition (Smith, 2002). When KLT is applied on a set of vectors which composes a dataset the number of the vectors are the same in the transformed domain with the original domain. On the other hand k number of vectors in the transformed domain, where k is less than the number of the vectors in the original domain, contains the high frequency components of the images as seen in Figure 3.3. It means that these vectors has high entropy and contains high volume of information.

Inverse transformation of the KLT transformed images does not need the all of the transformation output vectors. In this case the input vectors for the inverse transformation are choosed in an order with decreasing frequencies. The output vectors of the inverse transformation process similarity to the original vectors would be increase with higher number of input vectors and with higher correlation between the original vectors.

The number of eigenvectors seen in flow chart is equal to the number of input vectors. At that step choosing feature vectors with threshold, by choosing not all of the eigenvectors the resulting number of vectors is same with the number of eigenvectors used. With inverse transformation of these vectors the result is different from the original image so the transformation is lossy. The inverse transformation flow chart is below.

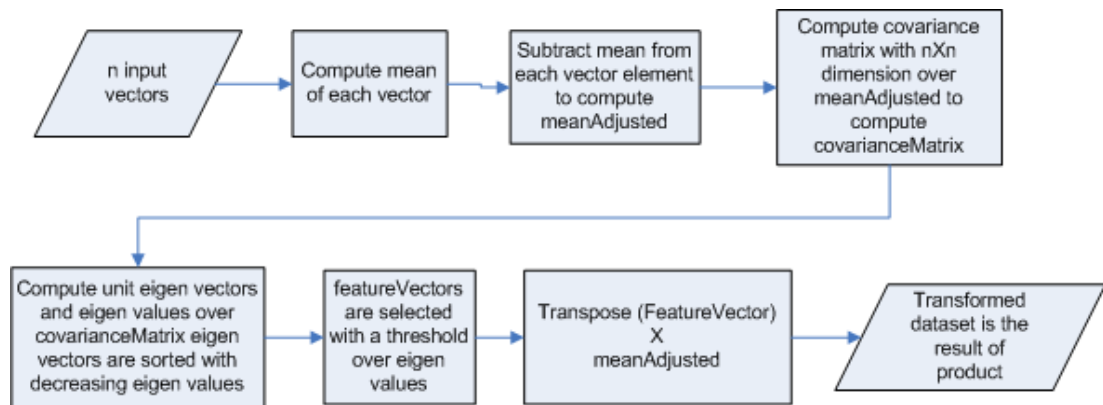


Figure 3.2 Flow chart of KLT

As seen KLT transforms n input vectors, where $n > 1$ to n output vectors. By the way the first step is the declaring the functions that is defining the vectors over the original dataset. The success of the transformation depends on the correlation between the vectors produced with the function. The number of the output vectors that contains the most of the information in the source would be decreased when the correlation between the input vectors are high.

Progressive image coding methods generally handles transmission of RGB images or gray level images. With KLT progressive encoding of images that has more bands would be transmitted. In this case user would choose the bands to composite RGB images for visualizing and remaining bands for analyzing during the transmission of the image. Thus without a new image request, changing the bands to visualize the dataset could be applicable with the incoming KLT components.

KLT is applied on Landsat images using the 7 different bands as seen in Figure 3.2. High correlation between different bands could easily detect directly with human visual perception. Therefore, the decomposition for producing vectors over source dataset could be performed over the bands. In this case transforming 7 bands of Landsat produce 7 output vectors. Performing inverse transformation with n vectors where n is between 0 and 7 all of the 7 bands which are not the same with original are reproduced. The result of the inverse transformation would be lossless when the all the vectors are used.

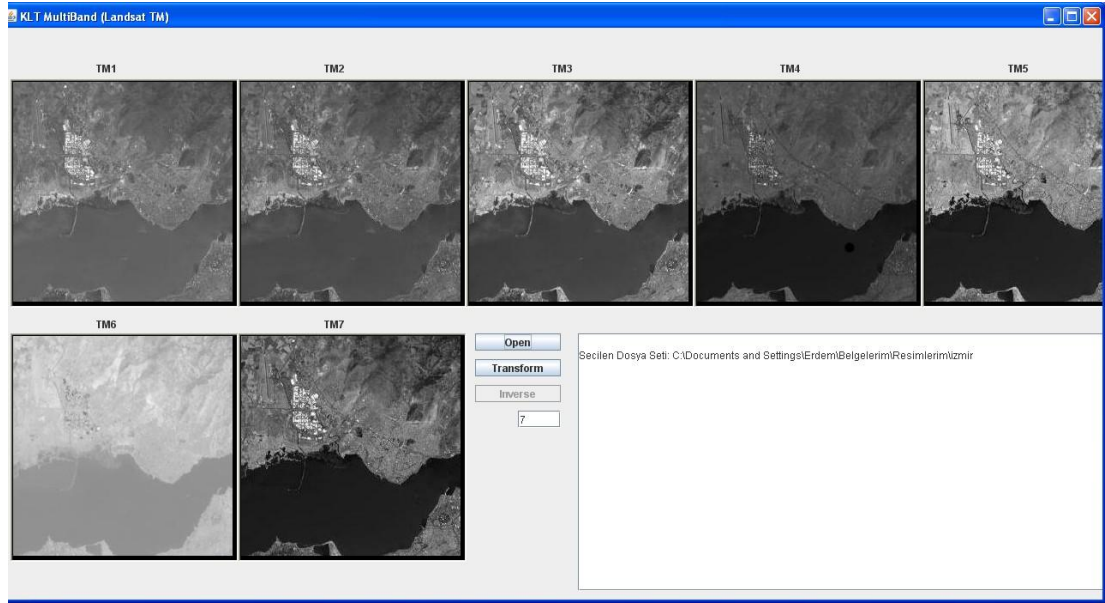


Figure 3.3 Landsat TM Images 7 bands to be transformed with KLT

The eigenvalues produced, which are seen in Table 3.1, after the transformation gives a clue about the lossy transformations similarity to the original. For example inverse transforming components that has Eigen values that are greater than 40 results have loss with none or low visual quality.

Table 3.1 Eigenvalues related with each components of Landsat TM 7 bands transformation

Component	Eigen Values
1	7630.19
2	651.66
3	103.11
4	73.65
5	58.98
6	38.89
7	18.50

The output components of KLT over Landsat TM 7 bands are seen in Figure 3.3 and the related eigenvalues are seen in Table 3.1. Objective image quality metrics, Signal to Noise Ratio (SNR) and Root Mean Square Error (RMSE), of the inverse transformation process with used number of components are seen in Tables 3.2 and 3.3. The ratio between the original image samples and the reproduced image samples

is called Signal to Noise Ratio. A transformed image has higher quality with higher SNR value than the image with lower SNR value. An infinite SNR value means a lossless transformation. RMSE is computed with the mean of each sample's distance to the original samples. A lower RMSE shows that the reproduced samples are closer to the original samples. Thus, a transformed image has higher quality than the image with higher RMSE. These metrics show that progressive image transmissions of multispectral images are achievable with KLT. Quality of each band increases after transmission of each component.

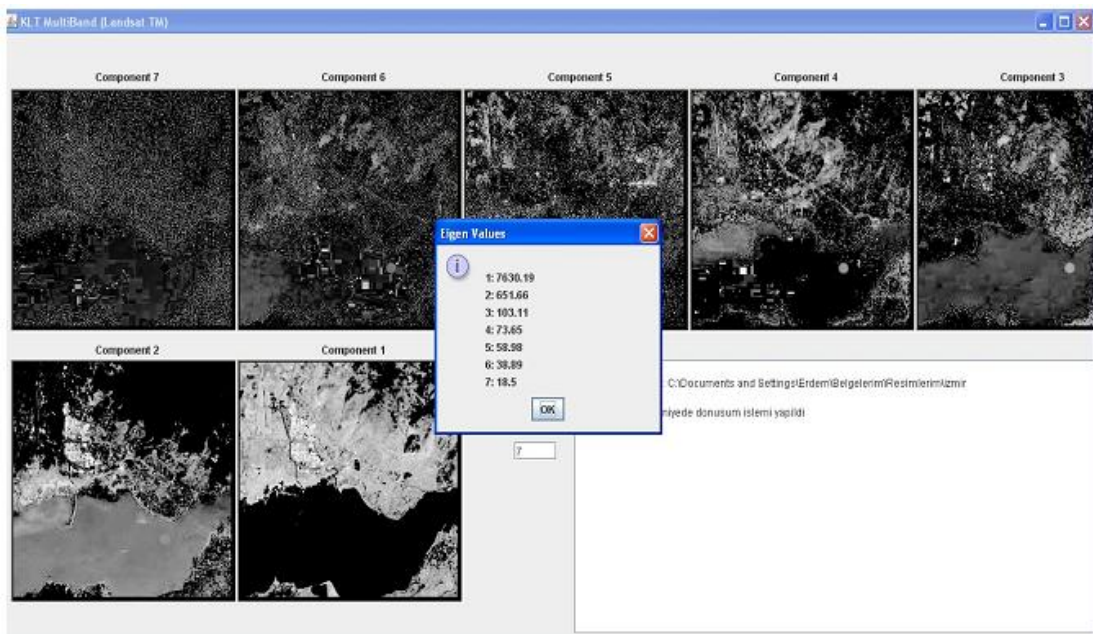


Figure 3.4 Landsat TM Images 7 components KLT transformation result

Table 3.2 SNR values of each band for number of components used

Number of Components Used	SNR Values for each 7 bands						
	1	2	3	4	5	6	7
1	18.16	17.92	19.41	16.20	20.41	22.90	20.09
2	27.81	26.41	25.60	18.20	26.68	27.83	20.34
3	28.23	27.91	25.94	21.67	26.68	27.87	27.30
4	28.23	27.91	27.74	25.07	26.94	33.88	28.93
5	28.62	28.17	28.78	31.03	34.56	43.19	39.76
6	31.61	29.87	48.52	46.06	63.38	83.68	54.91
7	∞	∞	∞	∞	∞	∞	∞

Table 3.3 RMSE values of each band for number of components used

Number of Components Used	RMSE Values for each 7 bands						
	1	2	3	4	5	6	7
1	3.63	12.75	11.69	10.31	10.69	12,80	8.58
2	4.52	4.68	5.75	8.22	5.22	7.27	8.34
3	4.31	3.94	5.54	5.54	5.22	7.23	3.76
4	4.31	3.94	4.51	3.75	5.06	3.63	3.11
5	4.12	3.82	4.00	1.89	2.11	1.24	0.9
6	2.92	3.14	0.42	0.34	0.08	0.02	0.16
7	0.00	0.00	0.00	0.00	0.00	0.00	0.00

As discussed above KLT transformation transforms vectors. Thus, input images have to be decomposed into vectors before transformation. Correlation between values in each vector, which has the same index, should be high for a better transformation results. In this case decomposition strategy, to produce vectors, is a significant process that directly affects transformation results. Generally columns or rows are chosen as vectors for single band transformation. However, it is trivial that this decomposition strategy is inefficient. Eigen Values of single band KLT with row order is seen in Table 3.4.

Table 3.4 Eigen Values of single band KLT with row order

Comp.	Eigen Value	Comp.	Eigen Value	Comp.	Eigen Value	Comp.	Eigen Value
1	7926.91	17	184.59	33	93.08	49	53.61
2	5357.98	18	177.56	34	89.48	50	52.7
3	2572.95	19	168.03	35	85.12	51	49.72
4	2300.33	20	165.19	36	84.51	52	47.93
5	982.9	21	158.41	37	77.77	53	45.86
6	634.3	22	143.55	38	74.55	54	43.2
7	553.15	23	139.2	39	72.97	55	42.4
8	464.54	24	135.41	40	70.82	56	41.9
9	387.04	25	130.84	41	69.99	57	40.97
10	352.69	26	123.29	42	69.52	58	35.91
11	295.66	27	117.65	43	67.53	59	34.98
12	281.97	28	111.83	44	62.39	60	34.41
13	255.1	29	106.37	45	61.21	61	28.14
14	249.54	30	104.57	46	60.7	62	25.25
15	216.22	31	97.22	47	58.45	63	24.75
16	205.61	32	93.95	48	57.39	64	21.92

A vector decomposition strategy is used to increase the correlation between vectors compared to column - row technique. Input image is divided into equal sized blocks. The number of vectors will be the number of samples in a block as seen in Figure 3.5. Block samples are distributed to each vector so each vectors sample with the same index is taken from the same block.

The vectors resulting with strategy declared over the example seen in Figure 3.5 would be take form as seen in Equation 3.6.



Figure 3.5 Vector determination function with resampling sample over single band

$$\begin{aligned}
V_1 &= [a_1, b_1, c_1, d_1, \dots, r_1, s_1] \\
V_2 &= [a_2, b_2, c_2, d_2, \dots, r_2, s_2] \\
V_3 &= [a_3, b_3, c_3, d_3, \dots, r_3, s_3] \\
V_4 &= [a_4, b_4, c_4, d_4, \dots, r_4, s_4] \\
&\dots\dots\dots \\
&\dots\dots\dots \\
V_n &= [a_n, b_n, c_n, d_n, \dots, r_n, s_n]
\end{aligned}
\tag{3.6}$$

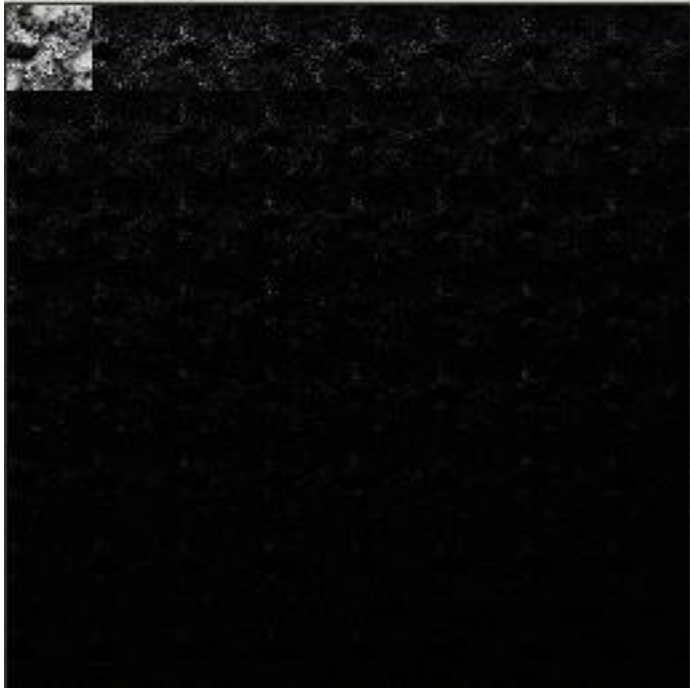


Figure 3.6 Landsat TM Image single component KLT transformation result

Eigen values resulting from transformation are seen in Table 3.5. Each Eigen value is related with an output component. An output component which has greater Eigen Value contains much more information from the original dataset. Lossy inverse transformation would be applied by using not all of the output components. The Eigen values are lower for each component as seen in Table 3.4 which contains row ordered vector transformation result.

Table 3.5 Eigen Values of single band KLT with resampling order

Comp.	Eigen Value	Comp.	Eigen Value	Comp.	Eigen Value	Comp.	Eigen Value
1	24994.87	17	0.66	33	0.09	49	0.09
2	1089.59	18	0.62	34	0.09	50	0.09
3	2925.44	19	0.14	35	0.09	51	0.08
4	339.12	20	0.13	36	0.09	52	0.08
5	129.82	21	0.12	37	0.09	53	0.08
6	85.47	22	0.11	38	0.09	54	0.08
7	61.54	23	0.11	39	0.09	55	0.08
8	49.01	24	0.11	40	0.09	56	0.08
9	31.13	25	0.1	41	0.09	57	0.08
10	29.0	26	0.1	42	0.09	58	0.08
11	14.79	27	0.1	43	0.09	59	0.08
12	12.19	28	0.1	44	0.09	60	0.08
13	2.24	29	0.1	45	0.09	61	0.08
14	1.33	30	0.1	46	0.09	62	0.08
15	1.23	31	0.09	47	0.09	63	0.08
16	0.72	32	0.09	48	0.09	64	0.08

A Landsat image with single component seen in Figure 3.5 which has width and height of 512 pixels. This image is divided into 64x64 sized blocks. Thus, there would be 64 vectors which would be transformed with KLT transformation. Each of the vectors contains 4096 samples. Each of 64 vectors is a downsampled image of the original image. These images are the principal components of the KLT. The resulting components' image representations are seen in Figure 3.7. These images are ordered with decreasing Eigen values from upper-left to lower-right. For progressive image transmission, these vectors would be served with declared order. The SNR of the images that are progressively produced are seen in Table 3.6.

Table 3.6 SNR Values of single band KLT for number of components used

num. of Comps.	SNR	num. of Comps.	SNR	num. of Comps	SNR	num. of Comps	SNR
1	20.12	17	27.01	33	32.21	49	40.12
2	20.94	18	27.32	34	32.57	50	40.70
3	21.80	19	27.65	35	32.95	51	41.34
4	22.32	20	27.97	36	33.36	52	42.02
5	22.79	21	28.26	37	33.78	53	42.81
6	23.26	22	28.57	38	34.25	54	43.63
7	23.67	23	28.88	39	34.71	55	44.52
8	24.02	24	29.19	40	35.18	56	45.53
9	24.39	25	29.53	41	35.66	57	46.77
10	24.74	26	29.85	42	36.16	58	48.49
11	25.07	27	30.18	43	36.71	59	50.7
12	25.42	28	30.50	44	37.23	60	52.32
13	25.74	29	30.85	45	37.79	61	54.63
14	26.05	30	31.19	46	38.38	62	57.79
15	26.36	31	31.52	47	39.00	63	62.7
16	26.68	32	31.85	48	39.55	64	∞

3.3 WAVELET TRANSFORMATION

Wavelet transformations over images are popular tools for image processing and multimedia compression applications. After transforming an image with wavelet transformation a multi-resolutional representation of the image is achieved. With wavelets a function space is decomposed into two parts; low frequency part that was spanned by scaling function and high frequency part that was spanned by wavelet function. Generally most of the information is carried by low frequencies. Thus, a multi resolutional representation of the dataset is produced by decomposing low frequency part, with wavelet transformation, recursively. As seen wavelet transformation provides frequency information of a dataset.

There are different transformations which produce frequency information like the Fourier Transformation. Fourier Transformation does not provide spatial information (time information) of the frequencies. Short Time Fourier Transformation (STFT) is

applied to obtain spatial information of the frequencies decomposed. Windowed blocks of the original data are transformed to apply STFT. Thus, the frequencies that has larger bandwidth from the window size will not be decomposed with this method. However wavelet transformation provides the time-frequency representation natively (Polikar, 2001).

With wavelet transformations, spatial information's resolution of the frequency components decomposed decreases with the frequency because of the higher spatial extent of the components which have higher band widths. Thus, by transforming low frequency components recursively dimension of the low frequency components are decreased, which carries the most of the information. Generally high frequency components are compressed better than low frequency components because of their lower entropy.

Discrete wavelet transformations (DWT) are used in different computing applications like image processing, multi-resolutional processing, and multimedia compression. The DWT analyzes the input data at different frequency bands with different resolutions by decomposing the data into a coarse approximation (Low frequency component) and detail information (High frequency component). DWT transformation is declared with two functions; scaling function, which is a low pass filter, and wavelet function, which is a high pass filter as seen at Equation 3.7.

$$\begin{aligned}
 y_{low}[k] &= \sum_n x[n] * g[2k - n] \\
 y_{high}[k] &= \sum_n x[n] * h[2k - n]
 \end{aligned}
 \tag{3.7}$$

A position-scale representation of the data is provided with by applying convolution (similar to Equation 3.7) over the low frequency component recursively, which is named sub-band coding. With each recursion low frequency components

each dimension and also resolution are decreased to half. The recursion process is seen in Figure 3.7. After transforming image with this process high frequency components has low energy as seen in Figure 3.8.

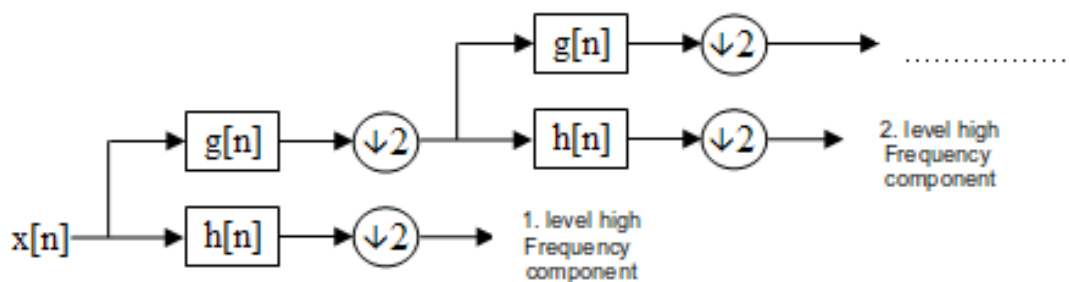


Figure 3.7 Subband Coding

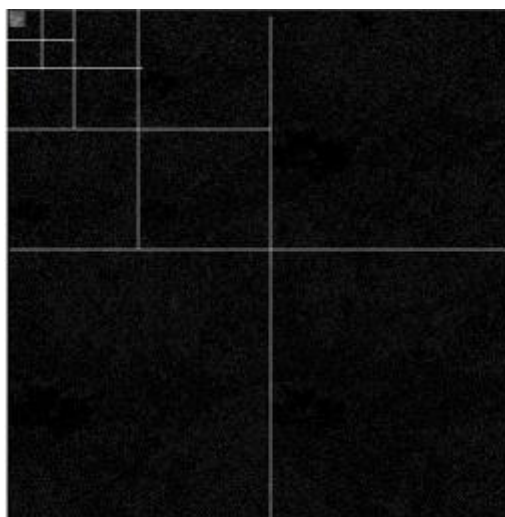


Figure 3.8 Wavelet Transformed Landsat TM Image from Izmir region

The Figure 3.8 is a result of wavelet transformation of the Figure 3.9, which has dimensions 512x512. Image is transformed with 5 recursions. Thus, the lowest resolution component dimension will be 16x16 (each dimension is divided with 2^5). Upsampled images SNR and RMSE after inverse transformation of each level is seen in Table 3.6



Figure 3.9 Single component of Landsat TM Image from Izmir region

One of most the popular way for DWT with integers is lifting schemes. Lifting schemes uses two basic functions while transformation and inverse transformation; predict and update as seen in Figure 3.10 and Figure 3.11 (Sweldens, 1995). Other functions for transformation used are addition, difference, split and merge. Thus update and predict functions that produce integer values provide integer transformation.

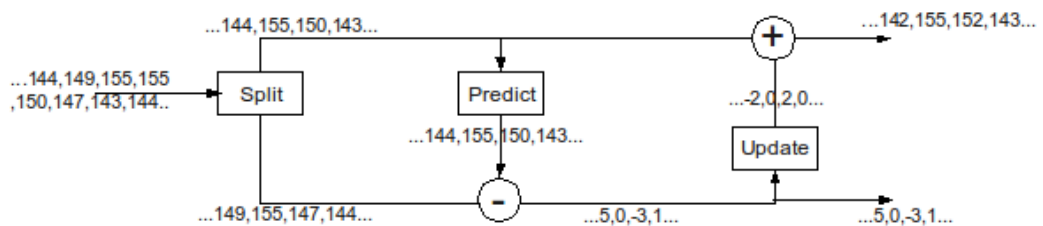


Figure 3.10 Forward transformation with lifting scheme

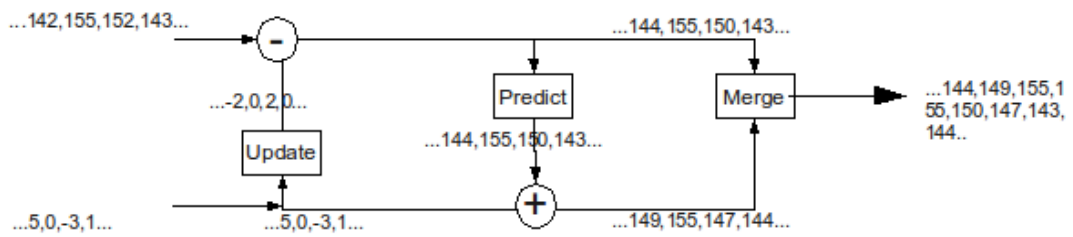


Figure 3.11 Inverse transformation with lifting scheme

During transformation first splitting the odd and the even indexed samples to produce two datasets are is applied over the input dataset. Then with predict function of DCT odd values are predicted from even values. The difference taken from the odd samples and predicted values. After that update function is applied to difference values. Finally these values are added to predicted values. The samples produced with addition are the low frequency component and the values produce by difference are the high frequency component. These steps are applied recursively for multiresolutional decomposition as declared in subband coding. Inverse transformation is performed with reversing the operations sequence and altering difference with add and add with difference. After that produced samples are merged to complete the inverse transformation. As figured predict and update operations are the key elements of the lifting schemes.

Image compression ratio is different for different wavelet filters as seen in Table 3.7. Transformation is applied with lifting schemes. At the table compressed file sizes are compared with each other and the png file containing the image. The file sizes of the PNG files are computed over single resolution, which does not provide a multi resolutional pyramid structure. Compressed image has the dimensions 2048x2048. Each wavelet resolution level is separated to quantize and compress to provide progressive transmissions.

Table 3.7 File Sizes of the Wavelet Transformed Lossless Compressed Pyramid Tile Bitsreams With JPEG 2000 and Non-hierarchical PNG Images

	W5X3	S(Haar)	WI4x2	WI4x4	WI2x4	PNG
Landsat-N36-1	4.3MB	6.2MB	10.4MB	9.3MB	4.1MB	12.1MB
Landsat-N36-2	3.4MB	6.1MB	9.8MB	8.8MB	3.4MB	11.2MB
escon-vnir	5.1MB	5.8MB	8.2MB	7.2MB	5.1MB	9.2MB
Landsat-1	2.9MB	4.0MB	7.3MB	6.4MB	2.7MB	7.3MB
Landsat-2	6.0MB	5.7MB	8.1MB	7.3MB	5.8MB	8.2MB
ortho-1	3.3MB	5.0MB	8.7MB	7.7MB	3.3MB	12.0MB
ortho-2	2.9MB	4.3MB	7.8MB	6.7MB	2.8MB	11.4MB
ortho-3	773.6KB	1.1MB	4.1MB	3.5MB	770.4KB	2.4MB
ortho-4	2.8MB	5.0MB	9.0MB	7.9MB	2.8MB	11.8MB
ortho-5	3.1MB	4.5MB	8.0MB	7.1MB	3.1MB	11.1MB
PiriReisReg	3.1MB	6.1MB	8.9MB	8.1MB	3.9MB	11.9MB
srtm-relief	2.2MB	2.5MB	4.7MB	4.0MB	2.2MB	5.5MB
DRG-250K-1	7.7MB	5.1MB	6.8MB	3.7MB	5.5MB	946.8KB
DRG-250K-2	8.5MB	6.3MB	7.3MB	4.3MB	6.7MB	1.2MB
DRG-250K-3	8.5MB	6.0MB	6.6MB	3.8MB	6.3MB	1016.5KB
WA-LANDSAT	8.5MB	6.0MB	6.6MB	3.8MB	6.3MB	8.9MB
wa-relief	1.4MB	2.3MB	5.7MB	4.9MB	1.4MB	6.5MB
bmng-1	4.1MB	4.3MB	6.3MB	5.4MB	4.2MB	5.7MB
bmng-2	4.9MB	5.0MB	6.9MB	6.0MB	5.0MB	6.9MB
bmng-3	2.3MB	3.1MB	7.3MB	6.3MB	2.3MB	7.4MB
bmng-4	2.4MB	3.3MB	2.4MB	6.4MB	2.4MB	8.5MB

CHAPTER 4

DEVELOPED METHODOLOGY FOR PROGRESSIVE TILE TRANSMISSION

Tiling image pyramids is a popular method to increase the performance of geospatial web services that serves geospatial images. OGC published a new standard, Web Map Tile Service (WMTS), which defines the interface between GIS server and clients that uses image tiles. Furthermore tiling enables server side caching as applied on GeoWebCache, which is an open source software project. In spite of performance improvement of tile services, redundant data transmission occurs that causes a load over the transmission network.

On the other hand non-redundant transmission of the image datasets could be provided with compression methods, which use wavelet transformation as the basis. JPEG 2000 image could be served with JPIP and ECW image could be served with ECWP protocols, which are defined in sections 1.2.2 and 2.2. These protocols provide non-redundant image transformation. However the whole dataset has to be transformed before any of the image transmission session. Datasets have to be imported to JPEG 2000 before serving them by the GIS server or have to be imported to ECW before serving them with ECWP.

In Chapter 3 it is seen that wavelet transformation provides a multi resolutional non-redundant transformed image data structure. In this thesis a tile caching mechanism with wavelet transformations are integrated to improve the performance

of geospatial image transmission. Wavelet transformation is used to decrease the redundancy for efficient use of the bandwidth and data storage. With this method whole dataset transformation is not required to transmit multi resolutional image parts. On server side tiling and caching is used to lower the load on the data source and reduce the computational time for transformation and compression of the response to the client queries. On the other hand client side caching should be used to decrease load on network. Also tiling provides easy to implement and high performance caching mechanism.

4.1 METHODOLOGY

Internet based geospatial image transmission is one of the critical elements of web GIS. The first step in a geospatial image transmission is sharing metadata. Coordinate reference system and geographic projection are the required metadata to request and visualize geospatial datasets. Raster datasets, especially high resolution datasets, are large in size. Visualizing such datasets, with a web based system, requires multi-resolutional spatial random access. Thus, indexing mechanisms have to be used to improve the performance to access regions on datasets. Other performance increasing methods used with tiling are ; client side caching to decrease the load on the network, server side caching to decrease the load on the data source, pre-fetching to decrease the time to display the subsequent regions with different or the same resolution with current tile.

Image transformations are the bases of the most popular image compression formats. DCT is used in JPEG, wavelet transformations are the basis of JPEG 2000, which has a wide usage area, like ECW and MrSID which are popular formats in GIS. KLT transformation is another image transformation that decomposes an image into different components with different and decreasing entropies. In addition to compression capabilities of the image transformation they could provide different types of quality layers. Wavelets provide highly scalable data structure, which is a

multi-resolutional leveled structure to access to the transformed image with coarser to detailed images. Wavelets are used to produce hierarchical and non-redundant structures to provide tile part images and differences to extract different resolutions.

Image pyramid tile indexes provide high performance access to large sized datasets. There are systems that use image pyramid tile images to serve datasets to GIS clients. However redundant data is transmitted from GIS server with different resolutions of a region. Transmitting differences between resolutions would decrease the redundancy. Indexing the differences with tile indexes provides efficient access to codeblocks. However, serving the differences for all levels would cause a high overhead caused by the required number of parent levels through to the root. To decrease the number of required parent levels code-blocks should contain differences the root with defined level intervals. Tiles should contain the differences from the current intervals root tile, which are covered by the parent tiles with increasing resolution. Thus, root tiles of intervals contain images and the remaining tiles contain differences from their parent tiles.

The flow chart of the developed methodology is seen in Figure 4.1. An abstract tiled image pyramid is constructed to index tile parts. After that each tile is transformed to produce sub-hierarchy.

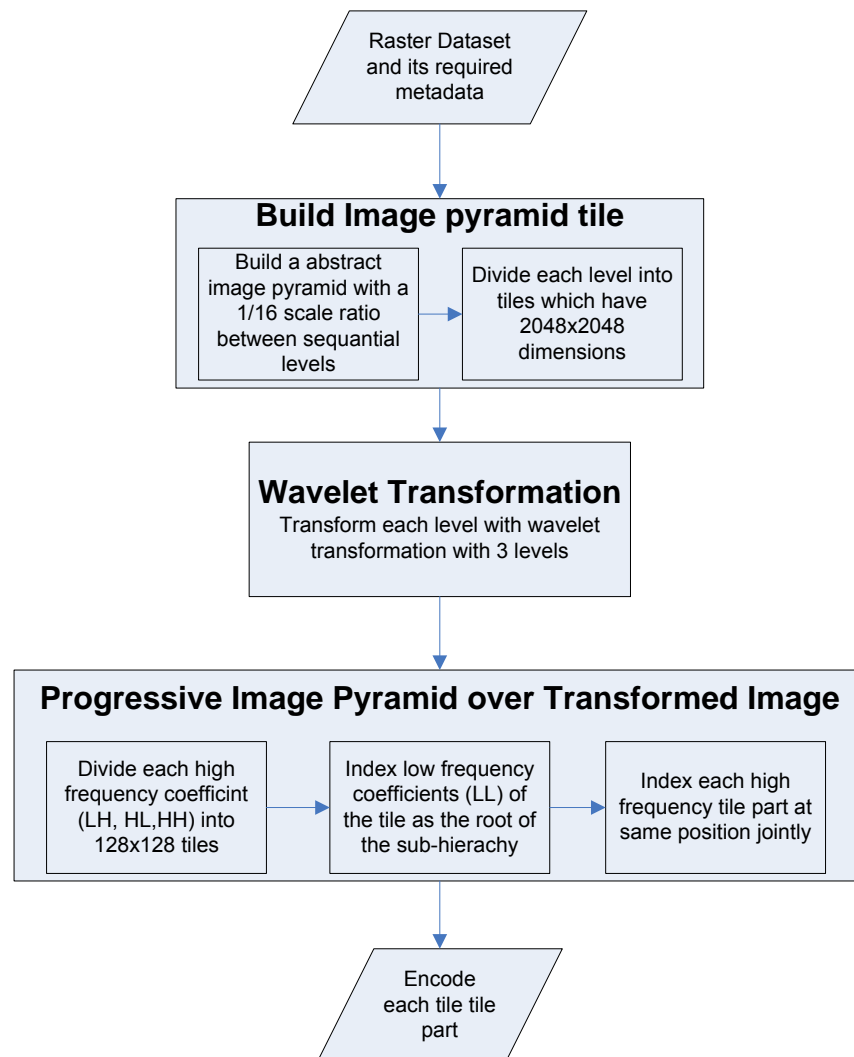


Figure 4.1 Flow chart of hybrid methodology developed for progressive image tiles

Image pyramid tiling and wavelet transformed image approaches both provides multi-resolutional access to large image datasets. Both of them have advantages and disadvantages. The affects of disadvantages could be decreased by integrating these methods. The integration of the methods builds a hybrid system. This system uses wavelet transformation as compression basis. The most important capability of the wavelet transformation is non-redundant multi-resolutional access. On the other hand tiled image pyramids are well organized multi resolutional accessible structures, which have high redundancy that causes an important load over the network. Organizing wavelet coefficients as tiled image pyramids provides an efficient

method to compute data blocks indexes to request and reconstruct the required sub-image.

Wavelet coefficients could be organized as image pyramid tile parts. However the number of the required tile levels to reconstruct the image from wavelet coefficients increases with the number of the wavelet transformation level. Therefore, wavelet transformation could be used to produce sub-levels of an image pyramid to decrease redundancy over the hierarchy. n number of wavelet transformations over an image provides $n+1$ hierarchical levels. Using transformations would decrease the number of image pyramid levels that has to be produced from the source dataset. Thus, the load over data source would be decreased. Producing tiles that covers wavelet coefficients provides easy to implement systems, which already use hierarchical map tiles.

Build Image Pyramid Tile and Wavelet Transformation components in Figure 4.1 are developed over an image tile pyramid hierarchy which has tiles with dimensions 256×256 . Tiles with sizes 256×256 are frequently used in internet mapping systems. 3 levels of transformation are applied over tiles. Thus, 4 sequential levels would be provided after transforming each tile part. Tile parts with dimensions 2048×2048 are processed to provide a single tile with dimensions 256×256 at lowest frequency after transformation which has 3 levels. During wavelet transformation it is observed that 3 levels of transformation are sufficient for a good compression ratio. Higher levels of transformation would provide better compression ratio however more number of transformations causes more computation time which would suffer web GIS server.

Progressive Image Pyramid over Transformed Image in Figure 4.1 which contains the whole wavelet coefficient at lowest frequency is providing to store and serve as a single tile. Higher frequencies are divided into 128×128 tile parts. These

tile parts, HH HL and LH, are merged to store and serve at same level according to their position to provide tiles at upper levels.

4.2 IMPLEMENTATION

GIS tile clients request tiles with their indexes. These indexes identify the tiles position and resolution. Thus, clients first requests the datasets metadata and tiling information to determine the hierarchy and the geographic projection of the dataset. This request has to be made at the beginning of the each geospatial data transmission session for each dataset that would be requested.

Each tile is cached at client side to provide tiles which covers the same position with better resolutions. Required tiles' indexes are computed to render the current tile image. The tiles which are required and are not cached are requested from the server. Each tile is indexed with x, the tile column position,y the tile row position and level the resolution level of the tile. Each tile that contains high resolution coefficients requires parent tiles. Parent tile of a requested tile to render is computed with **Algorithm 1. Requested Tile** is the current tile index that is requested from the server to render. **getX**, **getY** and **getLevel** returns the tile index values of a tile.

Algorithm 1 Finding parent tile: getParent(requestedTile)

```
parentX ← requestedTile.getX()/2  
parentY ← requestedTile.getY()/2  
parentLevel ← requestedTile.getLevel() – 1  
parentIndex ← createTileIndex(parentX,parentY,parentLevel)
```

Each tiles parent is computed and rendered recursively. Thus, rendering a specific tile requires a tile set. The required tile set is computed with the **Algorithm 2**. The tiles in the required tile list that are not cached at client would be requested to render the current tile. The **requiredTiles** data structure used in algorithm is a stack. In this step a sub-hierarchy of the whole hierarchy is determined to render the current tile.

Algorithm 2 Computing required tile set for requested tile

```
requiredTiles  $\leftarrow \emptyset$   
requiredTiles.push(curTile)  
curTile  $\leftarrow$  requestedTile  
while Mod(curTile.getLevel(), 4)  $\neq$  0 do  
    curTile = getParent(curTile)  
    requiredTiles.push(curTile)  
    curTile = getParent(requiredTile)  
end while
```

Parent tiles have 4 discrete children that covers a quarter of the parent. Thus, at step of gathering required tiles, prefetching is occurred for each sibling of child tiles in the sub-hierarchy requested. The entire parents in the requested sub-hierarchy are rendered recursively to render the requested tile. At each step of recursion the current parent region is computed with the children indexes which would be rendered. Recursive tile rendering algorithm is seen in **Algorithm 3**.

Tile is progressively rendered over the each element iteratively in the **requiredTiles** stack. **curTile** is the tile in the iteration. The coverage region of the **curTile** is computed over the parent image (**baseImage**). **ITransform** is the inverse transformation to produce the tile image with the parent image and the tiles coefficients. At the end of the iteration **resultImage** is the rendered tile image for the current tile index.

Algorithm 3 Recursive Tile Rendering

```
resultImage = requiredTiles.pop().getImageData()  
while requiresTiles.hasMoreElements() do  
    curTile = requiredTiles.pop()  
    curlImage = curTile.getImageData()  
    isNorth = Mod(curTile.getY(), 2)  
    isEast = Mod(curTile.getX(), 2)  
    baseImage = resultImage.getQuarterImage(isEast, isNorth)  
    resultImage = ITransform(baseImage, curlImage)  
end while
```

Wavelet transformation are implemented with integer lifting schemes are to transform images. Integer coding is used for low computational complexity and reversible transformation capabilities. Lifting filters with two steps are chosen for transformations that have low computational complexity. W5x3 which is applied in JPEG 2000 reversible coding scheme, S transform which is the integer lifting equalivent of Haar and interpolating lifting kernels with different sizes WI4x2, WI4x4 and WI2X4 are used.

Defined hierarchy is implemented over the GeoKIT SWS (Spatial Web Services) with Java under the GeoDB-imigi package. With the services implemented code blocks are served with their tile indexes. Tile parts produced are cached to decrease the transformation and response overhead for same tile and the other tiles which has the same root tile. A client module tor request and render the hierarchy is implemented over GeoKIT GeoObserver, which is a virtual globe application. Client module uses the cache structure of GeoObserver to render the tiles using their own and parents' codeblocks. The hierarchy is easily integrated with the existing systems because the existing server and clients have the capability to use image pyramid tile hierarchies. The general system view is seen at Figure 4.2.

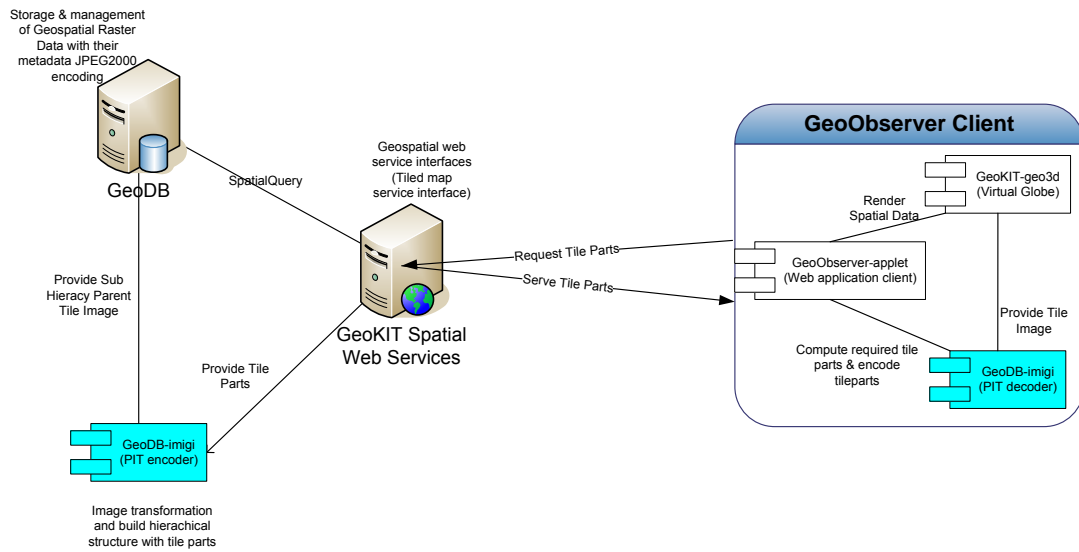


Figure 4.2 Architecture of the Developed Geospatial Image Transmission System

Implemented hierarchy is applied over nine different datasets. These datasets are presented at Appendix A. All of the images used have 8 bits radiometric resolution. Alpha bands are included during transformation and compression. JP2 and PNG format of the images are used to provide alpha bands. Thus, four bands of the images are transformed. Ortho images used have 0.5 meters, scanned DRG maps have 2.4 and Landsat images and Aster image (very near infrared bands) have 15 meters spatial resolutions.

Five integer lifting kernels are used for transformation. All of the transformation has just two lifting steps. Different kernels that have more lifting steps would have higher computational complexity. W5x3 that is used in JPEG 2000 images for reversible transformations, Haar transform, also its reversible integer transformation is known as S transform, and the interpolating kernels that has 2 lifting steps WI4x4, WI2x4 and WI4x2 (Calderbank, et al., 1998) (Sheng, et al., 1998) are used for transformation.

4.3 RESULTS AND DISCUSSIONS

Ordinary image pyramid tiling method is applied over the test datasets to compare with the progressive tile hierarchy. The resulting images are encoded with JPEG, PNG and JPEG 2000 formats. JPEG 2000 and PNG encoded tiles contains alpha band for transparency. Tile sets are compressed with 5 levels of transformation and a compression ratio 30 with JPEG 2000 encoding, which has resulting tile images that are visually lossless or near lossless. Total sizes of the hierarchies with different encodings of ordinary hierarchy and with different lifting kernels used for progressive tile hierarchies are seen in Table 4.1.

Total sizes of the hierarchies with different encodings of ordinary hierarchy and with different lifting kernels used for progressive tile hierarchies are given in Table 4.1. The number of tiles downloaded, for 5 different type of dataset, over a network with one megabit per second is seen in Figure 4.3. As seen in the Figure 4.3 number of tiles downloaded with JP2 encoded Progressive Image Tiles (PIT) are downloaded faster than the JP2 encoded tile images.

Transformed pyramid hierarchy is compressed with JPEG2000. Tiles that carry high frequency components of the images are compressed without wavelet transformation during compression. Thus, JPEG 2000 is used for quantization and entropy coding, not used for multi-resolutional coding. Different compression ratios are used for different levels in hierarchy. The compression ratios are chosen to get a total file size for hierarchy similar to ordinary hierarchy which is encoded with JPEG2000. After experiments compression ratio for progressive tile structure is formulated with the Equation 4.1. Tiles at parent levels are compressed with lower compression ratio because loss is inherited by the child tiles.

$$\begin{aligned} & \text{compressionRatio}(\text{level}) \\ & = \begin{cases} 1.35 * (3.5^{\text{level}}) & \text{if level is not equal to 0} \\ 0 & \text{if level is equal to 0} \end{cases} \end{aligned} \quad 4.1$$

Implemented transformations lossless and lossy compression capabilities are compared with each other and popular image compression formats. 5 different types of images from 9 different data sets are used in experiments. During lossless compression it is observed that WI2x4 transformed images are generally compressed with better compression ratio from the other data blocks which are transformed with other filters. The second filter that has the best compression ratio is W5x3. Some of the W5x3 transformed images have the same compression ratio WI2x4. WI4x4 has better performance on scanned maps during lossless compression. Lossless compression performances compared with the resulting data blocks sizes. On the other hand during lossy compression each filters results data blocks are compressed with same compression ratios. Thus, lossy compression performances are compared with objective quality metrics SNR at each tiles rendered from code blocks. It is observed that the W5x3 filter has the best performance over the lossy compressed geospatial images. W5x3 transformed hierarchies compressed with JPEG 2000 have better quality then the tiles compressed separately with JPEG and JPEG 2000.

The results are compared in Table 4.1 according to their sizes. However compression methods that are used to compress hierarchies are lossy methods. Objective image quality metrics could be used to compare the lossy compressed datasets. SNR is used to compare each kernel and each encodings performance. The tiles which are gathered directly from the datasource, are used as source image to compute SNR. SNR of progressive tile hierarchy tiles are compared with lossy compressed JPEG and JPEG 2000 images. Comparison of each datasets progressive tiles with JPEG images is seen in Table 4.3 and with JPEG 2000 images is seen in Table 4.2.

During losless compression, images that are transformed with WI2x4 (and for some cases, scanned maps, with WI4x4) are compressed with higher compression

Table 4.1 Lossy Compressed Image Tile Pyramid hierarchy Sizes

DATASETS	Wavelet Kernels Used to Transform Progressive Image Tiles Encoded with JP2 (KB)					File Formats to Encode Tile Image		
	W5X3	WI4x2	WI2x4	WI4x4	S-(Haar)	JPG	JP2	PNG
Landsat-N36-1	685.55	681.46	686.62	684.02	686.06	1.67MB	689.97KB	15.92MB
Landsat-N36-2	671.78	683.03	671.86	693.05	671.85	1.61MB	651.70KB	14.57MB
escon-vnir	684.41	677.90	682.42	679.26	683.09	1.50MB	686.98KB	15.09MB
Landsat-1	621.02	683.13	619.82	679.87	641.56	1.07MB	649.25KB	9.65MB
Landsat-2	685.91	679.50	687.47	677.95	685.16	1.15MB	690.08KB	10.55MB
ortho-1	680.36	684.39	678.74	682.40	683.85	1.11MB	687.92KB	15.45MB
ortho-2	684.19	684.53	686.24	682.38	684.32	692.39KB	1.11MB	14.14MB
ortho-3	514.61	667.79	514.73	642.92	540.72	295.21KB	537.91KB	3.35MB
ortho-4	673.35	687.03	673.21	684.95	682.76	1.18MB	690.21KB	15.49MB
ortho-5	683.05	683.03	684.58	677.97	680.56	1014.26KB	688.87KB	13.84MB
PiriReisReg	683.05	679.0	682.62	680.10	683.07	1.69MB	679.70KB	14.96MB
srtm-relief	622.64	677.75	625.92	664.83	621.06	885.11KB	885.11KB	6.90MB

Table 4.1 Continued

DATASETS	Wavelet Kernels Used to Transform Progressive Image Tiles Encoded with JP2 (KB)					File Formats to Encode Tile Image		
	W5X3	WI4x2	WI2x4	WI4x4	S-(Haar)	JPG	JP2	PNG
DRG-250K-1	685.70	682.49	684.61	681.13	686.71	2.64MB	690.27KB	3.80MB
DRG-250K-2	687.28	681.84	684.03	681.62	687.36	2.84MB	686.13KB	4.53MB
DRG-250K-3	686.28	683.08	686.93	679.27	683.93	2.60MB	689.76KB	4.17MB
WA-LANDSAT	686.66	686.61	688.13	684.49	688.34	840.03KB	692.88KB	11.86MB
wa-relief	649.51	680.54	654.51	667.69	660.36	696.03KB	686.02KB	8.37MB
bmng-1	687.85	686.34	687.99	684.70	683.59	615.01KB	694.98KB	7.34MB
bmng-2	688.69	685.12	688.61	684.75	686.77	714.45KB	693.76KB	8.85MB
bmng-3	680.76	685.93	679.50	684.42	685.20	710.19KB	687.48KB	9.53MB
bmng-4	683.60	686.14	681.09	681.87	684.78	808.56KB	688.53KB	10.81MB

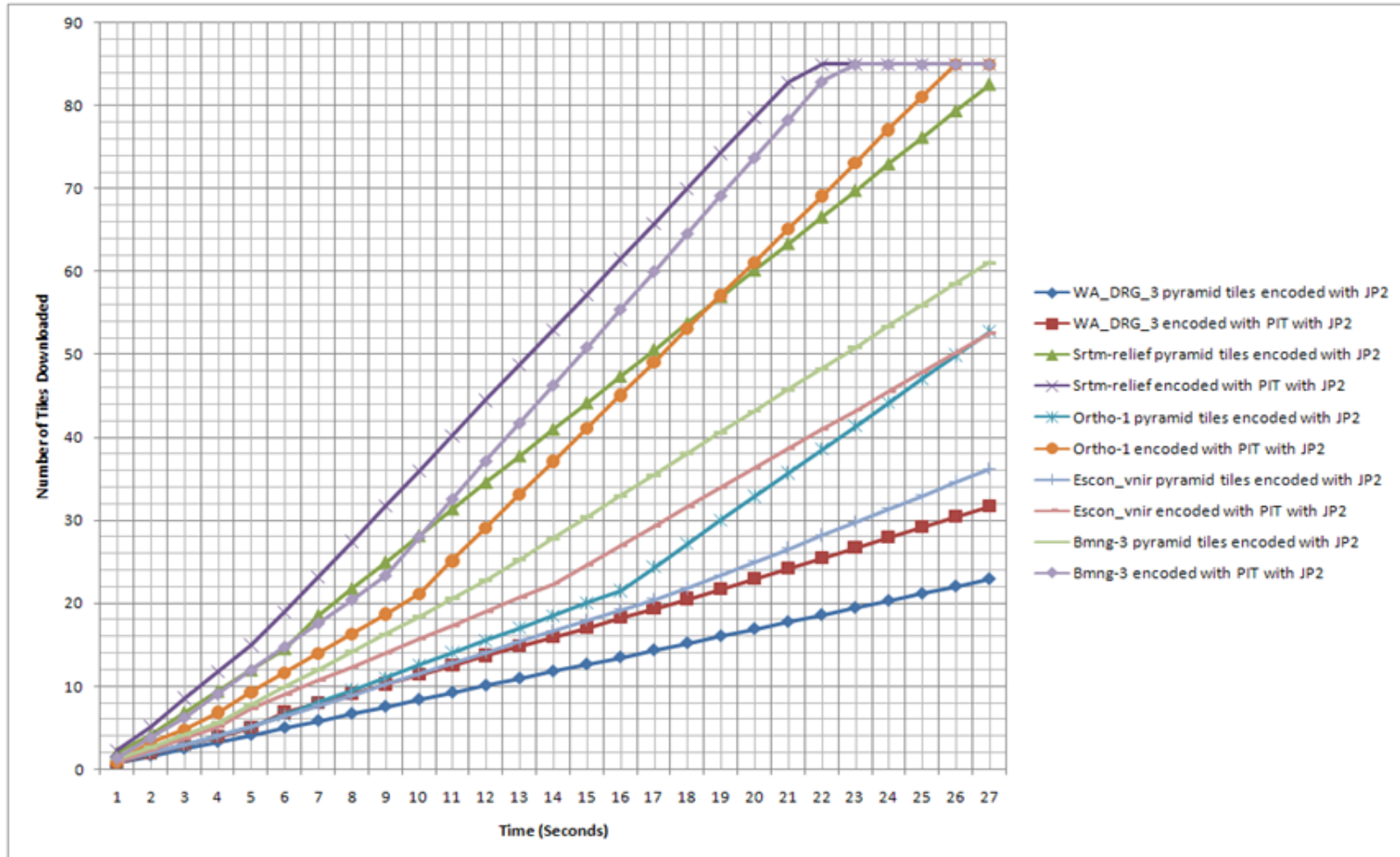


Figure 4.3 Lossless compressed JP2 encoded tiled image pyramids and JP2 encoded Progressive Image Tiles

ratio as seen in Table 3.7. However lossy compressed image tiles that are transformed with W5x3 have better quality than other kernels as seen in tables 4.2 and 4.3.

Table 4.2 Comparison of JPEG 2000 encoded Image Tile Pyramid and Progressive Image Tile Pyramid hierarchies SNR

Dataset	W5x3		Haar		W12x4		W4x4		W4x2	
	PIT	JP2	PIT	JP2	PIT	JP2	PIT	JP2	PIT	JP2
Landsat-N36-1	69	16	18	67	21	64	6	79	38	47
Landsat-N36-2	64	21	15	70	18	67	13	72	36	49
escon-vnir	70	15	18	67	14	71	20	65	26	59
Landsat-1	48	37	13	72	11	74	4	81	36	49
Landsat-2	26	59	19	66	11	74	2	83	3	82
ortho-1	81	4	20	65	14	71	13	72	77	8
ortho-2	64	21	17	68	17	68	17	68	54	31
ortho-3	34	27	22	63	21	64	8	77	34	41
ortho-4	46	39	18	67	21	64	5	85	25	60
ortho-5	77	8	17	68	11	74	15	70	60	25
PiriReisReg	68	16	13	71	21	63	4	80	19	65
srtm-relief	62	17	13	71	21	64	14	71	43	37
DRG-250K-1	65	20	63	22	21	64	20	65	48	37
DRG-250K-2	62	23	46	39	21	64	21	64	21	64
DRG-250K-3	63	22	54	31	22	63	14	71	10	75
WA-LANDSAT	40	45	22	63	21	64	9	76	20	65
wa-relief	68	17	21	64	21	64	6	79	62	23
bmng-1	56	29	66	19	4	81	5	80	36	49
bmng-2	55	30	51	34	6	79	6	79	23	62
bmng-3	57	28	23	62	5	80	5	80	46	39
bmng-4	67	18	25	60	10	75	6	79	57	28

As seen in Table 4.2 and 4.3 most of the tiles of progressive image tiles hierarchy has better quality than the tiles encoded with the JPEG 2000 and JPEG. JPEG 2000 encoded tiles which have better quality are produced from Landsat-2 and WA-LANDSAT images. The JPEG encoded tiles which have better quality than progressive image tiles are produced from the images DRG-250K-1, DRG-250K-2, DRG-250K-3, Landsat-N36-1, Landsat-2 and escon-vnir.

Table 4.3 Comparison of JPEG encoded Image Tile Pyramid and Progressive Image Tile Pyramid hierarchies SNR

Dataset	W5x3		Haar		WI2x4		W4x4		W4x2	
	PIT	JP2	PIT	JP2	PIT	JP2	PIT	JP2	PIT	JP2
Landsat-N36-1	21	64	0	85	18	67	4	81	13	72
Landsat-N36-2	69	16	0	85	10	75	2	83	29	56
escon-vnir	21	64	0	85	13	72	14	71	10	75
Landsat-1	51	34	29	56	10	75	7	78	41	44
Landsat-2	31	54	23	62	10	75	4	81	9	76
ortho-1	59	26	3	82	13	72	5	80	27	58
ortho-2	57	28	3	82	17	68	8	77	45	40
ortho-3	85	0	85	0	21	64	21	64	85	0
ortho-4	65	20	2	83	21	64	5	80	26	59
ortho-5	65	20	12	73	11	74	13	72	52	33
PiriReisReg	64	20	2	82	22	62	1	83	6	78
srtm-relief	53	32	30	55	23	62	24	61	52	33
DRG-250K-1	16	69	0	85	21	64	1	84	4	81
DRG-250K-2	17	68	0	85	21	64	0	85	0	85
DRG-250K-3	34	51	13	72	22	63	0	85	0	85
WA-LANDSAT	56	29	26	59	21	64	9	76	27	58
wa-relief	85	0	27	58	21	64	5	80	85	0
bmng-1	81	4	81	4	4	81	6	79	62	23
bmng-2	71	14	75	10	6	79	5	80	41	44
bmng-3	73	12	33	52	5	80	5	80	62	23
bmng-4	72	13	37	48	8	77	5	80	59	26

4.3.1 SCANNED MAPS

There are 4 scanned maps are used for experiments, 3 of them, DRG-250K-1, DRG-250K-2, DRG-250K-3, are extracted from 250K DRG map of Washington (U.S. State) (United States Geological Survey, The National Map Seamless Server, 2010) and the remaining one, PiriReisReg, is the scanned ancient Piri Reis map. Transformation coding best entropy decreasing field is natural images. However they have capability to compress drawings and computer graphics.

As seen in Table 4.1 scanned maps JPEG encoded tiles have relatively lower compression ratio. Thus, sub-hierarchies encoded with PIT are downloaded faster than the tile images that are encoded with other formats as seen in Figure 4.4. At the

beginning of the transmission JPEG 2000 encoded tile images are downloaded faster than the PITs. However, total time to download whole hierarchy with PIT is the minimum. On the other hand, JPEG encoded tiles have better quality than the progressive image tiles and JPEG 2000 encoded tiles because of their lower and constant compression ratio. It is clearly seen progressive tiles at hierarchy levels 0,1,2 have better quality than JPEG encoded tiles at Table 4.4. Progressive tiles at level 3 are coarser than the other encodings. However their SNR shows that they could be visually acceptable for a multi resolutional displaying environment.

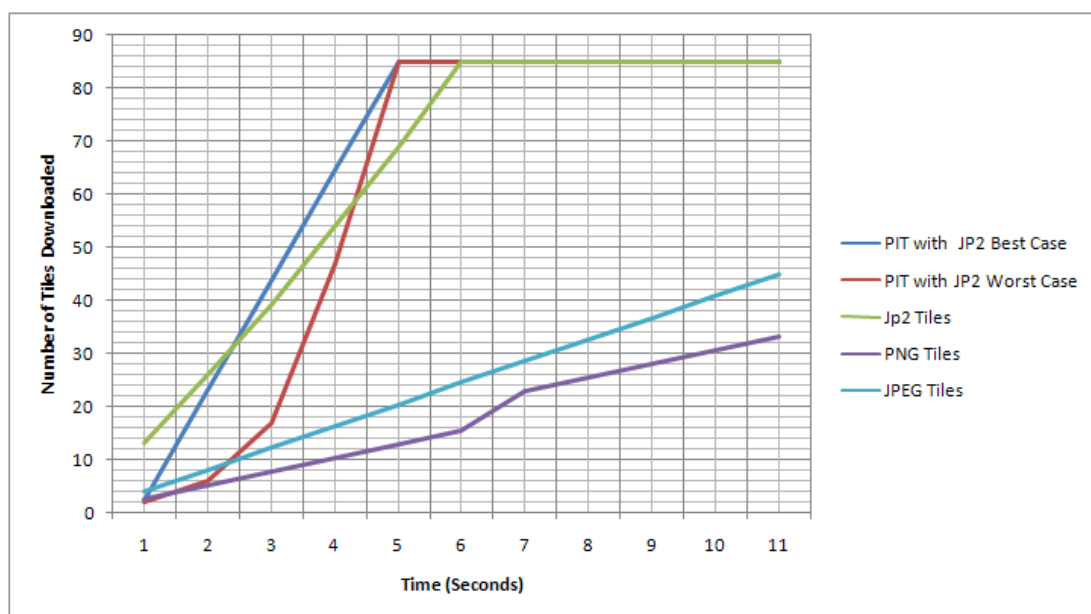


Figure 4.4 Number of tiles downloaded with 1Mbps of DRG-250K-3 image with different image pyramid hierarchies

Table 4.4 Lossy compressed DRG-250K-3 image JP2 JPEG and Progressive Tile Stream Based on W5x3 SNRs

Tile ID	Stream SNR	JPEG SNR	JPEG2000 SNR	Tile ID	Stream SNR	JPEG SNR	JPEG2000 SNR
1-1-1	93.610	39.403	26.566	3-2-7	40.542	44.925	40.170
1-1-0	90.696	38.537	27.074	3-3-1	57.458	51.532	59.747
1-0-1	72.375	33.262	21.154	3-2-6	29.461	37.242	28.102
1-0-0	146.444	53.206	41.785	3-3-0	51.226	49.334	52.974
0-0-0	126.868	38.154	26.538	3-2-5	30.763	37.869	32.327
3-7-7	47.930	48.975	48.355	3-2-4	34.251	40.866	32.878
3-7-6	45.571	47.943	45.564	3-2-3	39.897	43.581	37.084

Table 4.4 Continued

Tile ID	Stream SNR	JPEG SNR	JPEG2000 SNR	Tile ID	Stream SNR	JPEG SNR	JPEG2000 SNR
3-7-5	55.205	52.300	59.586	3-2-2	47.506	47.632	47.572
3-7-4	40.799	45.215	40.178	3-1-7	35.375	42.153	35.346
3-7-3	35.843	47.164	35.184	3-2-1	65.473	56.376	66.038
3-7-2	34.487	43.579	32.864	3-1-6	38.061	42.467	37.811
3-6-7	35.977	41.661	32.517	3-2-0	57.833	52.787	60.739
3-7-1	34.561	42.494	34.326	3-1-5	30.647	38.571	30.000
3-6-6	32.754	36.773	31.979	3-1-4	38.136	51.137	39.500
3-7-0	34.792	42.899	34.397	3-1-3	49.988	56.032	46.152
3-6-5	38.652	43.460	37.480	3-1-2	50.338	48.388	49.895
3-6-4	34.791	42.222	31.980	3-0-7	41.982	43.095	44.230
3-6-3	27.555	36.166	25.683	3-1-1	57.159	51.232	58.154
3-6-2	27.228	34.126	24.595	3-0-6	36.484	42.311	36.604
3-5-7	36.772	43.302	37.035	3-1-0	55.488	49.592	56.851
3-6-1	38.468	52.388	37.453	3-0-5	27.229	35.753	26.164
3-5-6	43.622	44.539	42.563	3-0-4	28.565	36.644	27.531
3-6-0	38.492	51.718	36.007	3-0-3	39.052	43.969	38.617
3-5-5	29.920	34.695	27.883	3-0-2	45.083	45.252	50.482
3-5-4	31.433	36.225	30.370	3-0-1	49.554	47.491	51.810
3-5-3	35.053	38.873	33.525	3-0-0	58.081	51.623	60.072
3-5-2	39.053	41.755	42.544	2-3-3	48.005	44.163	34.605
3-4-7	37.732	41.880	37.449	2-3-2	51.548	45.380	35.647
3-5-1	47.519	46.972	48.376	2-3-1	34.781	33.411	22.960
3-4-6	23.666	28.979	22.013	2-3-0	39.817	38.551	25.960
3-5-0	44.049	50.552	41.541	2-2-3	41.796	39.771	29.968
3-4-5	34.733	39.351	33.225	2-2-2	36.201	35.395	26.385
3-4-4	28.457	34.241	26.867	2-2-1	45.074	42.417	33.269
3-4-3	34.550	39.041	34.548	2-2-0	62.101	54.200	52.346
3-4-2	40.054	42.563	39.734	2-1-3	36.224	35.244	25.506
3-3-7	36.322	41.835	34.698	2-1-2	35.731	33.980	24.859
3-4-1	55.875	49.361	57.127	2-1-1	48.071	41.947	31.771
3-3-6	25.141	30.973	23.706	2-1-0	77.657	63.314	66.284
3-4-0	47.446	46.561	51.205	2-0-3	47.507	44.257	33.276
3-3-5	32.014	37.278	33.416	2-0-2	34.634	33.400	24.057
3-3-4	30.244	37.572	29.476	2-0-1	59.946	50.362	43.175
3-3-3	35.369	42.796	31.554	2-0-0	76.359	61.820	71.366
3-3-2	39.480	42.436	38.710				

4.3.2 HIGH RESOLUTION ORTHO IMAGES

There are 5 ortho-images, which have high resolution (0.5m), are used for experiments covers regions from Washington (U.S. State). These images are extracted from the data repositories of United States Geological Survey \cite{USGS}s. Ortho Image-1 covers a region that contains a settlement, Ortho Image-2 covers a rugged terrain, Ortho Image-3 covers a smooth region which contains single crater, Ortho Image -3 covers a forest region and Ortho Image 5 covers a hydrographic which contains an island. Ortho Image -1 and Ortho Image 2 contains much more high frequency components than the other ortho images.

As seen in tables 4.2 and 4.3 most of the progressive image tiles quality is better than the tile images encoded with other formats. Table 4.5 contains the SNR of each tile with each encoding. At first 3 hierarchy levels, 0,1,2, progressive image tiles has the best SNR values. Also most of the progressive image tiles at level 3 has better quality than other formats. As seen in Table 4.5 the difference between SNRs of the progressive image tiles and the other encoding type that has the best SNR is not greater than 2. This state shows that each progressive image tiles quality is sufficient. Additionally PITs are downloaded faster than the tile image encoded with other formats as seen in Figure 4.5.

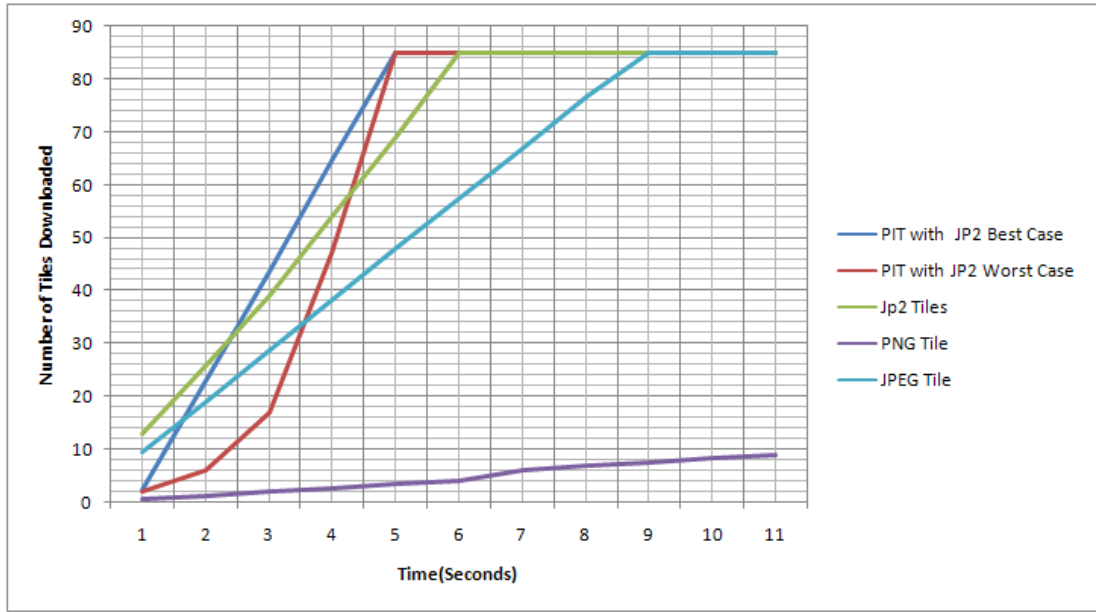


Figure 4.5 Number of tiles downloaded with 1Mbps of Ortho-Image-1 image with different image pyramid hierarchies

Table 4.5 Lossy compressed Ortho Image-1 image JP2 JPEG and Progressive Tile Stream Based on W5x3 SNRs

Tile ID	Stream SNR	JPEG SNR	JPEG2000 SNR	Tile ID	Stream SNR	JPEG SNR	JPEG2000 SNR
1-1-1	48.966	18.012	15.409	3-2-7	33.306	33.455	31.162
1-1-0	56.026	18.673	14.340	3-3-1	37.949	37.231	34.015
1-0-1	52.788	18.557	15.312	3-2-6	34.697	34.046	31.130
1-0-0	60.474	20.073	14.679	3-3-0	35.832	37.417	32.920
0-0-0	56.288	17.210	12.071	3-2-5	40.888	38.763	34.075
3-7-7	37.772	39.210	33.210	3-2-4	43.827	43.760	40.267
3-7-6	39.032	39.937	34.490	3-2-3	37.455	38.348	33.478
3-7-5	32.600	30.235	28.016	3-2-2	41.552	39.714	35.164
3-7-4	32.000	33.452	31.402	3-1-7	36.345	34.394	31.791
3-7-3	33.257	31.877	28.735	3-2-1	37.526	37.951	32.800
3-7-2	33.672	33.937	32.363	3-1-6	37.280	37.976	38.124
3-6-7	32.647	33.031	30.002	3-2-0	43.981	44.465	39.497
3-7-1	36.017	37.043	30.557	3-1-5	36.767	35.384	33.469
3-6-6	32.860	32.094	29.383	3-1-4	36.453	35.942	31.483
3-7-0	41.758	42.480	36.021	3-1-3	37.151	38.225	33.801
3-6-5	33.392	33.147	29.929	3-1-2	41.882	43.081	40.118

Table 4.5 Continued

Tile ID	Stream SNR	JPEG SNR	JPEG2000 SNR	Tile ID	Stream SNR	JPEG SNR	JPEG2000 SNR
3-6-4	34.418	34.673	31.881	3-0-7	34.888	33.118	31.447
3-6-3	31.619	32.040	28.678	3-1-1	36.967	36.044	31.615
3-6-2	36.805	35.911	31.839	3-0-6	37.301	36.014	31.226
3-5-7	34.167	32.952	28.465	3-1-0	38.417	38.970	34.315
3-6-1	40.798	41.882	35.889	3-0-5	35.130	35.328	34.190
3-5-6	32.269	32.401	32.963	3-0-4	29.066	28.720	26.140
3-6-0	42.448	41.986	36.600	3-0-3	43.712	42.477	39.008
3-5-5	24.901	27.146	29.911	3-0-2	49.381	47.084	42.568
3-5-4	32.157	29.890	27.300	3-0-1	37.679	37.981	33.488
3-5-3	38.072	35.045	32.353	3-0-0	37.947	38.904	34.849
3-5-2	37.988	39.764	34.311	2-3-3	38.308	23.797	19.320
3-4-7	37.062	33.763	30.750	2-3-2	35.920	22.799	19.925
3-5-1	40.913	40.834	35.347	2-3-1	36.847	22.383	19.030
3-4-6	30.532	30.488	30.748	2-3-0	44.405	27.076	20.408
3-5-0	42.336	43.071	39.439	2-2-3	35.975	21.863	19.285
3-4-5	30.852	29.705	27.507	2-2-2	32.644	20.786	19.038
3-4-4	34.464	34.160	31.731	2-2-1	36.931	22.573	17.040
3-4-3	32.829	31.069	28.852	2-2-0	43.846	26.618	20.484
3-4-2	28.704	28.324	23.731	2-1-3	37.212	23.020	19.742
3-3-7	37.963	34.898	32.362	2-1-2	43.606	26.475	22.254
3-4-1	39.889	38.675	34.575	2-1-1	42.499	25.780	21.048
3-3-6	39.065	38.804	36.427	2-1-0	41.452	25.875	19.781
3-4-0	41.595	40.790	36.554	2-0-3	38.183	23.748	20.601
3-3-5	42.255	40.716	36.608	2-0-2	36.885	22.929	19.432
3-3-4	40.814	39.691	37.189	2-0-1	46.039	28.182	22.347
3-3-3	40.890	38.378	36.195	2-0-0	40.274	24.803	19.183
3-3-2	39.744	39.141	39.726				

4.3.3 SHADED RELIEFS

Two shaded reliefs are used, which are digitally produced from the elevation data. One of them is extracted from the high resolution Washington (U.S.) National Elevation Dataset from (United States Geological Survey, The National Map Seamless Server, 2010), and the other one is extracted from SRTM data which covers a region from Himalayas. Progressive image tile encodings efficiency is very

high as seen from high SNR values at Table 4.6. In addition PITs are downloaded faster than the tile image encoded with other formats as seen in Figure 4.6.

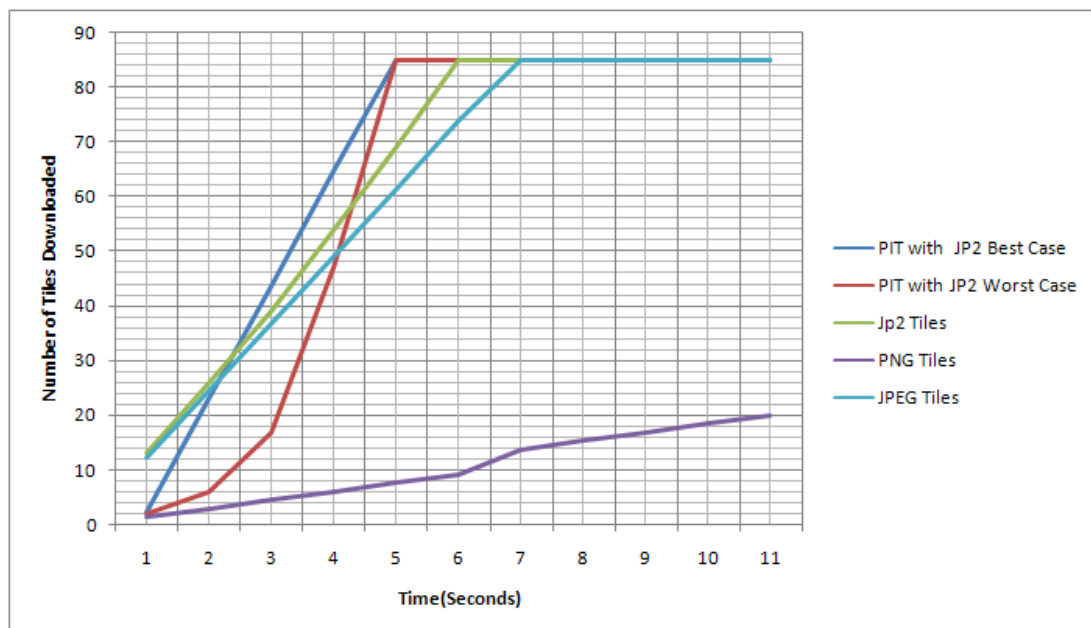


Figure 4.6 Number of tiles downloaded with 1Mbps of Srtm-Relief image with different image pyramid hierarchies

Table 4.6 Lossy compressed Srtm-relief image JP2 JPEG and Progressive Tile Stream Based on W5x3 SNRs

Tile ID	Stream SNR	JPEG SNR	JPEG2000 SNR	Tile ID	Stream SNR	JPEG SNR	JPEG2000 SNR
1-1-1	Infinity	54.733	42.972	3-2-7	71.563	82.340	64.592
1-1-0	Infinity	89.219	104.907	3-3-1	Infinity	259.834	Infinity
1-0-1	2.196.533	49.938	41.286	3-2-6	65.885	83.306	65.852
1-0-0	Infinity	84.077	103.241	3-3-0	Infinity	698.767	Infinity
0-0-0	Infinity	62.290	59.313	3-2-5	74.308	90.171	72.975
3-7-7	93.010	97.133	92.661	3-2-4	64.220	78.633	60.528
3-7-6	75.485	86.278	67.661	3-2-3	113.774	86.515	86.660
3-7-5	79.170	99.779	78.977	3-2-2	237.156	144.849	187.378
3-7-4	73.134	90.079	70.740	3-1-7	96.954	86.142	77.722
3-7-3	79.278	98.174	76.120	3-2-1	29.209.505	257.093	Infinity
3-7-2	68.824	78.931	61.844	3-1-6	113.893	96.318	94.800
3-6-7	82.261	100.771	89.762	3-2-0	Infinity	463.150	Infinity
3-7-1	152.082	89.130	96.100	3-1-5	79.702	86.985	69.868
3-6-6	95.932	107.540	89.183	3-1-4	78.946	84.403	71.732

Table 4.6 Continued

Tile ID	Stream SNR	JPEG SNR	JPEG2000 SNR	Tile ID	Stream SNR	JPEG SNR	JPEG2000 SNR
3-7-0	1.120.667	408.608	1.369.855	3-1-3	110.657	96.303	94.185
3-6-5	73.815	90.686	75.747	3-1-2	117.774	96.532	100.766
3-6-4	74.741	94.183	75.895	3-0-7	118.043	97.082	104.986
3-6-3	83.735	89.824	76.884	3-1-1	156.889	112.298	122.468
3-6-2	77.188	88.934	85.806	3-0-6	183.691	136.102	189.400
3-5-7	106.059	117.795	95.172	3-1-0	125.714	96.024	102.361
3-6-1	2.154.842	575.647	Infinity	3-0-5	91.308	94.249	95.518
3-5-6	100.476	114.134	95.869	3-0-4	85.000	89.239	80.241
3-6-0	1.951.970	458.664	Infinity	3-0-3	155.945	127.801	144.002
3-5-5	66.206	81.718	64.953	3-0-2	202.281	168.271	208.911
3-5-4	65.358	83.140	65.023	3-0-1	157.951	127.820	146.819
3-5-3	97.599	85.679	75.572	3-0-0	167.398	125.958	165.995
3-5-2	247.360	164.034	229.087	2-3-3	104.619	63.643	52.811
3-4-7	93.096	104.368	94.029	2-3-2	88.193	60.463	47.377
3-5-1	48.749.445	360.601	Infinity	2-3-1	92.163	57.401	46.033
3-4-6	95.891	108.675	84.324	2-3-0	2.266.802	175.267	272.329
3-5-0	Infinity	223.956	Infinity	2-2-3	117.036	69.855	64.768
3-4-5	68.313	86.567	69.143	2-2-2	75.336	53.569	42.361
3-4-4	61.177	75.290	57.616	2-2-1	204.985	72.945	78.307
3-4-3	95.826	76.921	75.042	2-2-0	Infinity	276.148	2.493.146
3-4-2	230.110	150.578	232.404	2-1-3	81.752	56.778	43.951
3-3-7	73.505	88.377	73.941	2-1-2	79.794	53.165	41.342
3-4-1	Infinity	250.913	Infinity	2-1-1	270.977	90.189	112.951
3-3-6	73.083	98.117	79.410	2-1-0	Infinity	333.831	3.168.213
3-4-0	Infinity	295.358	Infinity	2-0-3	165.663	66.603	68.851
3-3-5	70.292	85.206	68.394	2-0-2	101.778	56.932	48.158
3-3-4	67.824	77.894	64.216	2-0-1	199.058	73.998	79.099
3-3-3	242.715	153.624	216.033	2-0-0	203.059	76.343	83.816
3-3-2	259.381	164.258	233.263				

4.3.4 ALTERNATIVE COMPOSITIONS OF SATELLITE IMAGES

5 different RGB compositions of LANDSAT images and a composition of ASTER image of Escondida Mine (National Aeronautics and Space Administration Visible Earth A catalog of NASA images and animations of our home planet, 2010) which

contains visible and near infrared bands are used for experiments. WA-LANDSAT image is a false color LANDSAT composition from (United States Geological Survey, The National Map Seamless Server, 2010). Landsat-1, Landsat-2, Landsat-N36-1, Landsat-N36-2 images are gathered from (NASA GeoCover Data set, 2010). Band mapping of images from (NASA GeoCover Data set, 2010) are Band 7 (mid-infrared light) is displayed as red, Band 4 (near-infrared light) is displayed as green, Band 2 (visible green light) is displayed as blue.

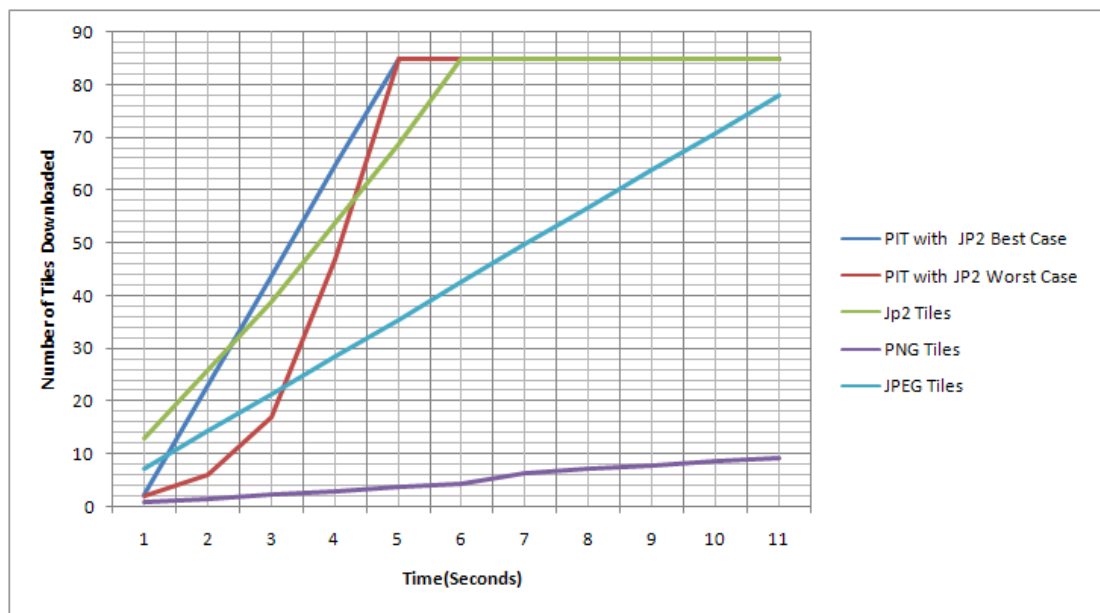


Figure 4.7 Number of tiles downloaded with 1Mbps of Escon-vnir image with different image pyramid hierarchies

Both 3 encoding methodologies performances are not as good as normal RGB compositions. This is caused by the RGB - YUV, reversible component transformations low performances on the images that have alternative band mappings. These color transformations are designed for RGB images. However quality of the tile images are sufficient for a multiresolutional displaying system as seen from SNR values of each tile at Table 4.7.

Table 4.7 Lossy compressed Escon-vnir image JP2 JPEG and Progressive Tile Stream Based on W5x3 SNRs

Tile ID	Stream SNR	JPEG SNR	JPEG2000 SNR	Tile ID	Stream SNR	JPEG SNR	JPEG2000 SNR
1-1-1	56.280	18.008	14.196	3-2-7	15.562	23.928	16.055
1-1-0	56.793	18.405	14.523	3-3-1	18.990	25.341	18.744
1-0-1	56.252	18.861	12.720	3-2-6	16.086	23.869	15.778
1-0-0	62.205	19.736	15.184	3-3-0	24.987	31.781	23.451
0-0-0	69.803	18.468	14.128	3-2-5	17.605	25.722	16.338
3-7-7	19.529	23.460	15.535	3-2-4	15.565	26.025	17.074
3-7-6	18.542	21.901	17.455	3-2-3	25.922	38.042	25.234
3-7-5	22.943	27.333	22.850	3-2-2	20.125	29.624	19.436
3-7-4	22.928	26.184	21.226	3-1-7	15.849	23.929	16.568
3-7-3	16.990	22.350	17.248	3-2-1	18.424	24.631	16.523
3-7-2	14.706	19.428	14.846	3-1-6	18.205	27.801	16.788
3-6-7	16.008	19.918	15.428	3-2-0	17.340	22.851	15.930
3-7-1	22.934	26.596	22.834	3-1-5	16.817	25.309	16.060
3-6-6	23.981	30.118	25.443	3-1-4	18.135	24.763	16.981
3-7-0	19.706	23.915	18.271	3-1-3	20.709	26.622	18.860
3-6-5	24.342	28.277	22.914	3-1-2	20.542	26.152	19.784
3-6-4	26.592	30.130	26.034	3-0-7	15.894	23.742	16.593
3-6-3	20.777	25.734	19.213	3-1-1	16.287	22.043	15.037
3-6-2	17.552	22.874	17.311	3-0-6	17.963	26.017	16.727
3-5-7	17.519	23.765	16.823	3-1-0	14.828	20.490	13.817
3-6-1	23.429	27.297	23.519	3-0-5	17.529	24.412	16.653
3-5-6	18.543	25.200	17.110	3-0-4	16.516	23.394	15.851
3-6-0	18.941	24.928	20.380	3-0-3	19.444	25.591	19.170
3-5-5	19.917	25.679	19.073	3-0-2	20.296	26.755	21.008
3-5-4	20.558	28.168	19.683	3-0-1	18.619	24.191	18.461
3-5-3	24.728	34.987	24.391	3-0-0	18.836	24.532	19.161
3-5-2	20.215	28.318	19.899	2-3-3	22.792	15.903	13.157
3-4-7	18.375	25.544	17.473	2-3-2	28.769	19.538	17.791
3-5-1	17.984	23.405	16.448	2-3-1	20.055	15.237	12.211
3-4-6	23.403	33.010	21.240	2-3-0	24.973	17.655	15.596
3-5-0	17.465	22.572	18.315	2-2-3	23.589	18.636	13.488
3-4-5	21.287	30.173	20.810	2-2-2	26.622	20.972	15.813
3-4-4	25.447	35.577	24.191	2-2-1	32.866	27.567	18.649
3-4-3	35.405	49.560	31.482	2-2-0	21.771	16.126	12.689
3-4-2	29.368	41.786	28.808	2-1-3	21.760	18.829	12.624

Table 4.7 Continued

Tile ID	Stream SNR	JPEG SNR	JPEG2000 SNR	Tile ID	Stream SNR	JPEG SNR	JPEG2000 SNR
3-3-7	18.947	26.925	17.687	2-1-2	26.205	24.806	15.809
3-4-1	20.417	25.919	18.369	2-1-1	33.754	28.486	20.079
3-3-6	21.769	31.873	20.340	2-1-0	23.604	17.909	14.059
3-4-0	15.622	20.781	15.705	2-0-3	20.308	17.929	12.221
3-3-5	27.526	39.861	24.621	2-0-2	21.114	17.405	11.993
3-3-4	31.180	47.376	32.589	2-0-1	25.076	17.906	15.028
3-3-3	32.865	45.861	29.312	2-0-0	20.695	16.108	12.218
3-3-2	37.047	50.583	37.894				

4.3.5 BLUE MARBLE NEXT GENERATION

The Blue Marble Next Generation (BMNG) is a series of cloud-free, global-scale images. It is created with processing over NASA Terra MODerate resolution Imaging Spectroradiometer (MODIS) science data collected in 2004. 4 images from BMNG are used, 2 of them covers Turkey and 2 of them covers The Globe. Progressive image tiles of BMNG images have high SNR that which is seen in tables 4.2, 4.3 and 4.8.

As seen in Figure 4.8 the number of the tiles encoded other than PIT downloaded at the beginning of the transmission is much more. However these tiles have lesser quality than the tiles images provided with PIT sub-hierarchy as seen in Table 4.8.

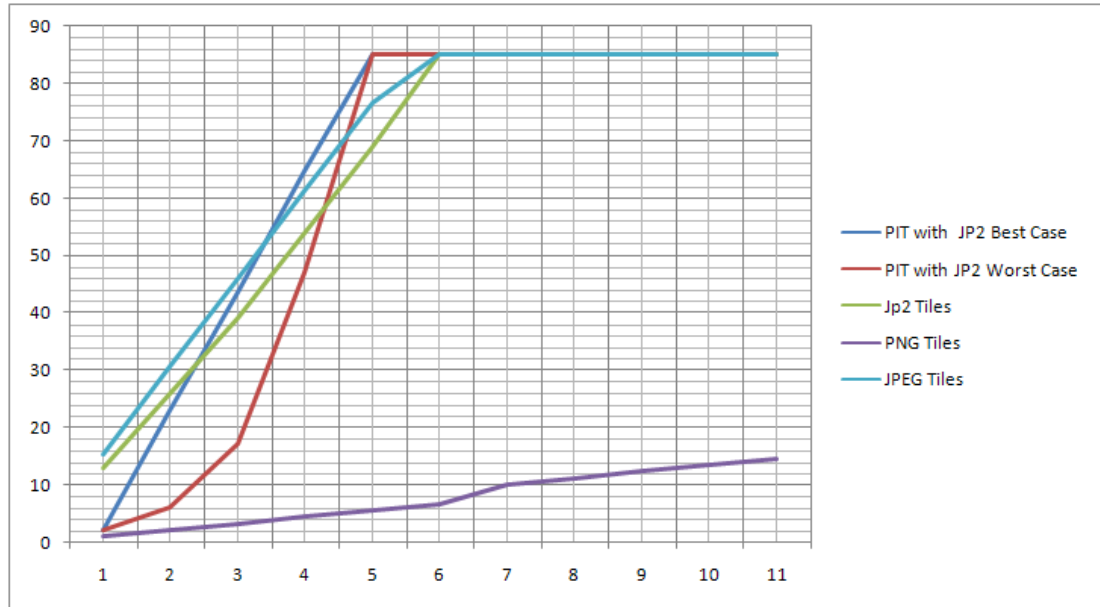


Figure 4.8 Number of tiles downloaded with 1Mbps of Bmng-3 image with different image pyramid hierarchies

Table 4.8 Lossy compressed Bmng-3 image JP2 JPEG and Progressive Tile Stream Based on W5x3 SNRs

Tile ID	Stream SNR	JPEG SNR	JPEG2000 SNR	Tile ID	Stream SNR	JPEG SNR	JPEG2000 SNR
1-1-1	68.729	16.477	14.854	3-2-7	42.177	42.190	44.616
1-1-0	80.974	20.469	21.263	3-3-1	48.544	42.756	41.938
1-0-1	58.770	14.213	13.803	3-2-6	27.129	22.189	21.681
1-0-0	62.654	15.070	15.118	3-3-0	49.779	57.410	151.788
0-0-0	65.567	13.382	12.605	3-2-5	25.305	23.837	23.551
3-7-7	25.473	22.201	24.033	3-2-4	25.116	22.370	22.366
3-7-6	31.258	26.970	25.409	3-2-3	24.474	22.647	23.827
3-7-5	38.861	39.556	40.449	3-2-2	34.959	30.818	35.609
3-7-4	41.478	38.078	38.951	3-1-7	31.105	26.520	27.414
3-7-3	34.493	29.647	26.041	3-2-1	44.076	29.140	37.515
3-7-2	32.864	29.100	21.761	3-1-6	33.203	29.081	32.851
3-6-7	39.006	39.673	13.172	3-2-0	53.185	56.488	214.320
3-7-1	53.232	35.097	48.636	3-1-5	27.595	26.733	38.686
3-6-6	27.317	23.094	22.158	3-1-4	31.694	28.209	36.319
3-7-0	64.800	57.993	142.975	3-1-3	33.507	26.550	33.911
3-6-5	37.995	36.091	34.469	3-1-2	42.677	36.049	57.144
3-6-4	34.787	30.228	28.328	3-0-7	23.267	19.598	19.810

Table 4.8 Continued

Tile ID	Stream SNR	JPEG SNR	JPEG2000 SNR	Tile ID	Stream SNR	JPEG SNR	JPEG2000 SNR
3-6-3	29.291	24.576	22.810	3-1-1	34.693	26.736	32.180
3-6-2	57.668	57.426	82.808	3-0-6	28.689	32.342	38.888
3-5-7	41.733	39.221	23.910	3-1-0	40.661	42.115	68.911
3-6-1	102.134	121.745	161.408	3-0-5	30.143	36.552	51.231
3-5-6	27.529	23.628	22.336	3-0-4	37.605	36.331	48.788
3-6-0	78.027	78.655	Infinity	3-0-3	28.563	23.424	27.217
3-5-5	31.110	31.168	29.235	3-0-2	49.134	44.763	104.387
3-5-4	30.898	30.048	26.807	3-0-1	37.215	29.281	33.544
3-5-3	28.942	27.858	24.828	3-0-0	49.757	55.073	123.043
3-5-2	29.777	26.032	29.256	2-3-3	34.572	18.496	17.345
3-4-7	35.058	34.158	43.622	2-3-2	44.251	24.508	22.372
3-5-1	86.337	82.046	127.030	2-3-1	43.088	20.925	20.358
3-4-6	26.762	22.364	22.380	2-3-0	79.492	41.230	70.355
3-5-0	64.479	51.147	219.818	2-2-3	36.095	19.339	18.243
3-4-5	30.612	26.519	25.005	2-2-2	33.415	19.663	17.665
3-4-4	32.030	31.968	29.798	2-2-1	34.218	17.753	16.582
3-4-3	28.657	25.010	22.521	2-2-0	77.705	46.529	81.952
3-4-2	29.886	26.143	33.366	2-1-3	38.089	20.198	20.514
3-3-7	36.397	31.928	37.093	2-1-2	30.089	17.293	16.005
3-4-1	78.341	66.902	290.381	2-1-1	32.862	16.250	16.131
3-3-6	32.333	28.110	30.631	2-1-0	53.087	30.190	40.106
3-4-0	60.988	40.684	123.914	2-0-3	32.983	18.060	17.892
3-3-5	28.553	28.396	24.973	2-0-2	36.014	22.732	24.981
3-3-4	29.242	29.191	26.696	2-0-1	44.547	20.498	22.957
3-3-3	25.484	21.175	20.923	2-0-0	47.675	23.614	27.060
3-3-2	27.451	24.464	29.561				

CHAPTER 5

CONCLUSIONS AND RECOMENDATIONS

A data structure developed to provide geospatial image transmission with high performance is seen in Section 4.1. This structure provides an encoding mechanism for multi-resolution random access. This access is provided with tile image pyramids tile indexes. With this property developed methodology could be integrated easily with current GIS systems that use web tile services.

Minimum requirements to develop a system that serve geospatial raster datasets are determined. The minimum metadata that has to be managed and served by the GIS server are coordinate reference system of the datasets, dimension of the datasets and geographical projection information of the datasets. The storage management which is used by GIS server has to provide multi resolutional random access seamlessly over the GIS raster datasets, which has high volume because of their dimensions.

Wavelets are the transformation which provides multi resolutional structure as seen in Section 3.3. Wavelet transformations are decreasing entropy of images that is important to increase compression ratio. Thus, wavelet transformed images have a well defined structure which could be integrated with image pyramids to decrease redundant data transmission.

Developed methodology produces wavelet coefficients. These coefficients are compressed with JPEG 2000 with parameterized factors as seen in Section 4.2. Parameters used in this thesis are chosen to supply file sizes. They are similar to tiled image pyramid sizes which are compressed with JPEG 2000. With these parameters quality of the tiles encoded with developed methodology are better than the tiled image pyramids encoded with JPEG 2000 and other file formats as seen in Section 4.3. On the other hand compression parameter could be changed to provide image tiles with different qualities. Additionally different entropy coding schemes or image compression formats could be used other than JPEG 2000.

Developed structure is implemented with Java as seen in Appendix B. Five different kernels for wavelet transformations are implemented with integer lifting schemes to transform images. Additionally methods implemented to build the tile hierarchy structure over the wavelet transformed image coefficients. Tiled image pyramids are recently used structures used in web GIS. Thus, developed system could be easily integrated with GIS software packages developed with java and support tiled image pyramids.

JPIP protocol could be wrapped with progressive image tiles interfaces. This would be simplifying to integrate JPIP technology with GIS application that already use web map tile services. Each sub hierarchy's parent tile image would be encoded with JPEG 2000 to serve sub hierarchy with JPIP. Image has to be encoded as a single tile during JPEG 2000 encoding. Priciencts are used within JPIP similar to tile parts in PIT. Thus, priciencts dimensions should be choosed similar to tile parts dimensions.

At the implementation of the developed methodology tile sizes of the abstract structure are chosen with dimensions 2048x2048. Three levels of wavelet transformation are applied over the tiles to provide 256x256 (that are frequently used in GIS applications) with a 4 levels of sub hierarchy. Tile dimensions and number of

transformation level could be changed to provide different structure with different properties.

Karhunen Loewe Transformation which is an examined transformation other than wavelet transformation in this thesis could be used to decrease redundancy of the multispectral images. On the other hand KLT could be applied over single bands with different input strategies. Row based or similarly column based strategies are inefficient methods. Different vector producing should be developed to increase the performance as it seen in Section 3.2

REFERENCES

- Beaujardiere, J. d. (2004, January). OGC Web Map Service Interface. Open GIS Consortium Inc.
- Bettio, F., Gobbetti, E., Marton, F., & Pintore, G. (2007). High-quality networked terrain rendering from compressed bitstreams. In *Web3D '07: Proceedings of the twelfth international conference on 3D web technology* (pp. 37-44). Perugia, Italy: ACM.
- Calderbank, A. R., Daubechies, I., Sweldens, W., & Yeo, B.-L. (1998). Wavelet Transforms That Map Integers to Integers. *Applied and Computational Harmonic Analysis*, 5 Number 3, 332 - 369.
- Daubechies, I. (1992). *Ten lectures on wavelets*. Philadelphia, PA, USA: Society for Industrial and Applied Mathematics.
- Geographic information -- Metadata -- XML schema implementation. (2007). Geographic information -- Metadata -- XML schema implementation. International Standards Organization.
- Geographic information - Metadata. (2003). Geographic information - Metadata. International Standards Organization.
- Geographic information -- Schema for coverage geometry and functions. (2005). Geographic information -- Schema for coverage geometry and functions. International Standards Organization.
- Herring, J. R. (2006, October). OpenGIS Implementation Specification for Geographic information - Simple feature access -Part 1: Common architecture. Open GIS Consortium Inc.
- Hu, S. Y., & Tao, V. (July, 2004). Use Image Streaming Technologies to Present High Resolution Images on The Internet. In *Geo-Imagery Bridging Continents* (Vol. XXXV, p. 1138). ISPRS.
- Hu, Y. (2004). *A Web-based two-dimensional/three dimensional geospatial image visualization system. Master Thesis*. York University (Canada).
- Kim, J. K., & Ra, J. B. (2004). A real-time terrain visualization algorithm using wavelet-based compression. *Vis. Comput.*, 20 Number 2, 67-85.

- Komzák, J., & Slavík, P. (2003). Scaleable GIS Data Transmission and Visualisation. In *IV '03: Proceedings of the Seventh International Conference on Information Visualization* (p. 230). Washington, DC, USA: IEEE Computer Society.
- Kyle, M., Burggraf, D., Forde, S., & Lake, R. (2006, January). GML in JPEG 2000 for Geographic Imagery (GMLJP2) Encoding Specification. Open GIS Consortium Inc.
- Maso, J., Pomakis, K., & Julias, N. (2010, April). OpenGIS Web Map Tile Service Implementation Standard. Open GIS Consortium Inc.
- Merzhausen, C. U. (2001). Wavelet based ECW image compression.
- Portele, C. (2007, August). OpenGIS Geography Markup Language (GML) Encoding Standard. Open GIS Consortium Inc.
- Prandolini, R., & Taubman, D. S. (2003). Architecture, philosophy, and performance of JPIP- internet protocol standard for JPEG2000. (T. Ebrahimi, & T. Sikora, Eds.) *Visual Communications and Image Processing 2003*, 5150 Number 1, 791-805.
- Sheng, F., Bilgin, A., Sementilly, P. J., & Marcellin, M. W. (1998). Lossy And Lossless Image Compression Using Reversible Integer Wavelet Transforms. In *Proc. of ICIP 1998* (pp. 876-880).
- Sweldens, W. (1995). The Lifting Scheme: A New Philosophy in Biorthogonal Wavelet Constructions. In *Wavelet Applications in Signal and Image Processing III* (pp. 68-79).
- Taubman, D. S., & Marcellin, M. W. (2001). *JPEG 2000: Image Compression Fundamentals, Standards and Practice*. Norwell, MA, USA: Kluwer Academic Publishers.
- Tu, S., He, X., Li, X., & Ratcliff, J. J. (2001). A systematic approach to reduction of user-perceived response time for GIS web services. In *GIS '01: Proceedings of the 9th ACM international symposium on Advances in geographic information systems* (pp. 47-52). Atlanta, Georgia, USA: ACM.
- Wu, J., Amaratunga, K., & Chitradon, R. (2001). Design of a Distributed Interactive Online GIS Viewer by Wavelets. *Journal of Computing in Civil Engineering* .
- Yang, P., Wong, C., David, Yang, R., Kafatos, M., & Li, Q. (2005). Performance-improving techniques in web-based GIS. *International Journal of Geographical Information Science* , 19 Number 3, 319-342.
- Yun Q. Shi, Huifang Sun. (1999). *Image and video compression for multimedia engineering : fundamentals, algorithms, and standards*. Boca Raton, Florida: CRC Press.
- Ze-Nian Li, Mark S. Drew. (2004). *Fundamentals of Multimedia*. New Jersey: Prentice Hall.

ONLINE REFERENCES

Accelerating WebGIS with Image Web Server. *Accelerating WebGIS with Image Web Server*. Retrieved June 2010, from www.resmap.com/pdf/acceleratingwebgis.pdf

GeoWebCache is a cache for WMS tiles implemented in Java. *GeoWebCache is a cache for WMS tiles implemented in Java*. Retrieved June 2010, from GeoWebCache is a cache for WMS tiles implemented in Java: <http://geowebcache.org/trac>

NASA GeoCover Data set. (2010, June). *NASA GeoCover Data set*. Retrieved from <https://zulu.ssc.nasa.gov/mrsid/>

National Aeronautics and Space Administration Visible Earth A catalog of NASA images and animations of our home planet. *National Aeronautics and Space Administration Visible Earth A catalog of NASA images and animations of our home planet*. Retrieved June 2010, from <http://visibleearth.nasa.gov/>

Polikar, R. (2001, January). *The Wavelet Tutorial*. Retrieved June 2010, from <http://users.rowan.edu/~polikar/wavelets/wttutorial.html>

Smith, L. I. (2002). *A tutorial on Principal Components Analysis*. Retrieved August 2010, from http://www.cs.otago.ac.nz/cosc453/student_tutorials/principal_components.pdf

United States Geological Survey, The National Map Seamless Server. *United States Geological Survey, The National Map Seamless Server*. Retrieved June 2010, from <http://seamless.usgs.gov/>

World files for raster datasets. *World files for raster datasets*. Retrieved June 2010, from http://webhelp.esri.com/arcgisdesktop/9.3/index.cfm?id=3046&pid=3034&topicname=World_files_for_raster_datasets

APPENDIX A

TEST IMAGE DATASETS

Test images used are extracted from 9 datasets, which are publicly available.

Data Set-I LANDSAT image that uses bands 7 (mid-infrared light) 4 (nearinfrared light) 2 (visible green light) (NASA GeoCover Data set, 2010)

Data Set-II False color LANDSAT image (United States Geological Survey, The National Map Seamless Server, 2010)

Data Set-III Escondida Mine ASTER image that contains visible and near infrared bands (National Aeronautics and Space Administration Visible Earth A catalog of NASA images and animations of our home planet, 2010)

Data Set-IV Digital Elevation Model of Washington State (United States Geological Survey, The National Map Seamless Server, 2010)

Data Set-V SRTM Elevation Data of World

Data Set-VI High resolution ortho images of Washington State (United States Geological Survey, The National Map Seamless Server, 2010)

Data Set-VII Blue Marble Next Generation images (National Aeronautics and Space Administration Visible Earth A catalog of NASA images and animations of our home planet, 2010)

Data Set-VIII DRG 250K scanned maps of Washington State (United States Geological Survey, The National Map Seamless Server, 2010)

Data Set-IX Scanned Piri Reis Map



Figure A.1 Istanbul Landsat Image 1



Figure A.2 Istanbul Landsat Image 2



Figure A.3 LANDSAT-N36-1 Image



Figure A.4 LANDSAT-N36-2 Image



Figure A.5 WA State LANDSAT



Figure A.6 Escon-vnir Image



Figure A.7 WA State Relief



Figure A.8 SRTM Relief



Figure A.9 Ortho Image 1



Figure A.10 Ortho Image 2



Figure A.11 Ortho Image 3



Figure A.12 Ortho Image 4



Figure A.13 Ortho Image 5

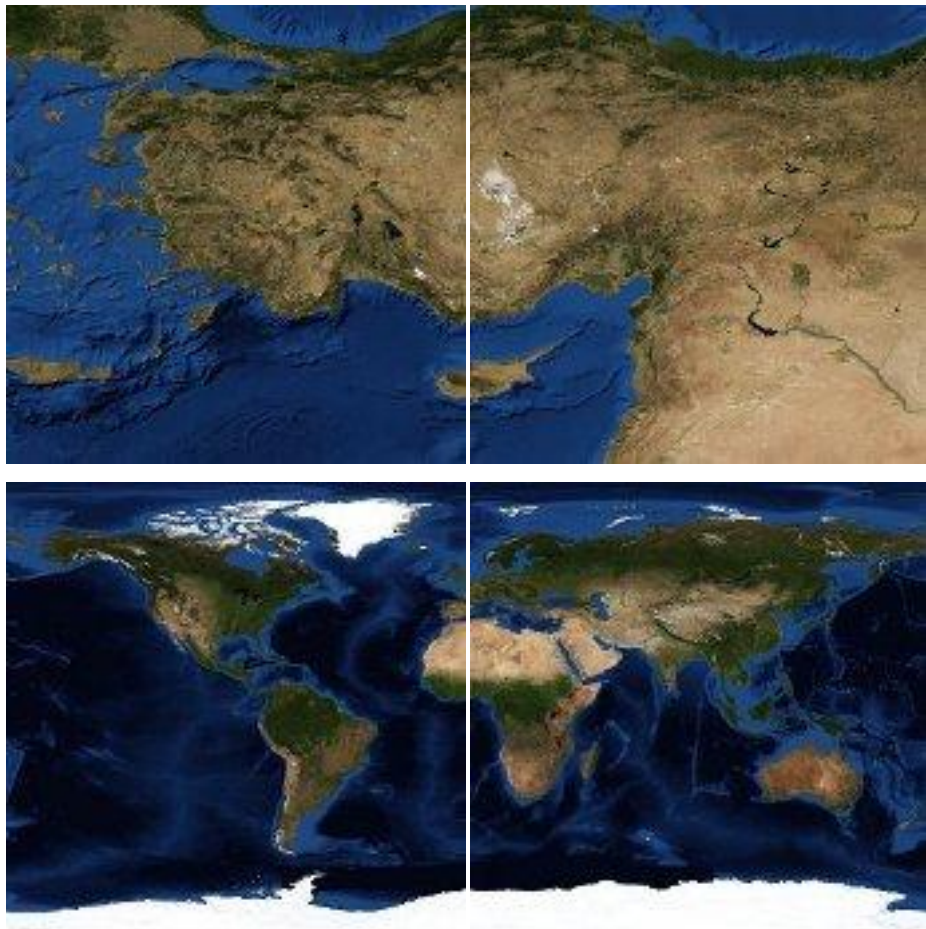


Figure A.14 Blue Marble Next Generation Image



Figure A.15 DRG 250K Image1

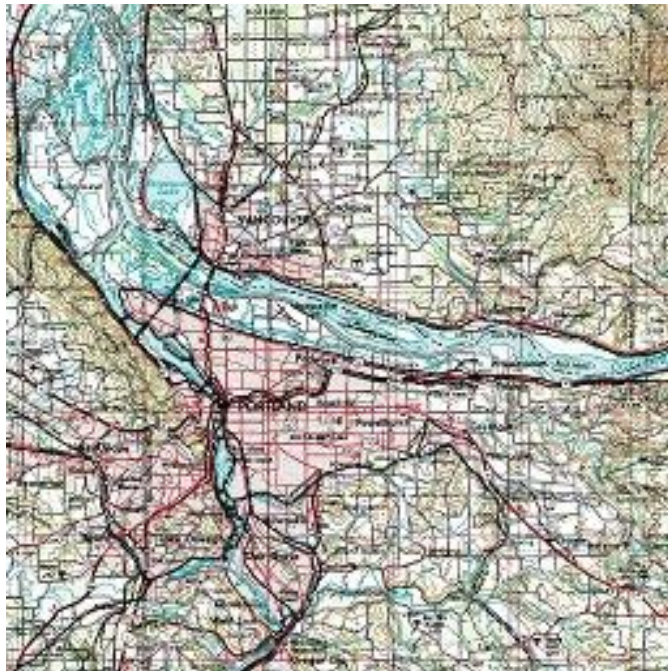


Figure A.16 DRG 250K Image 2

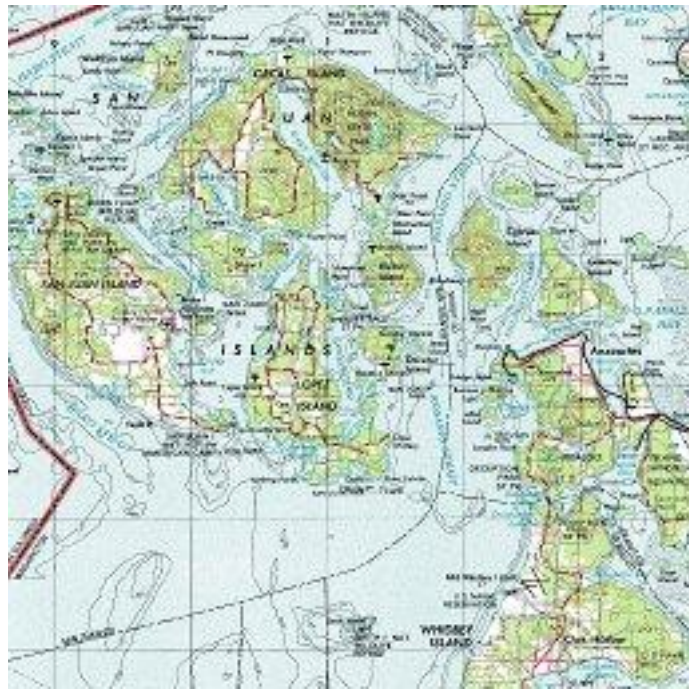


Figure A.17 DRG 250K Image 3

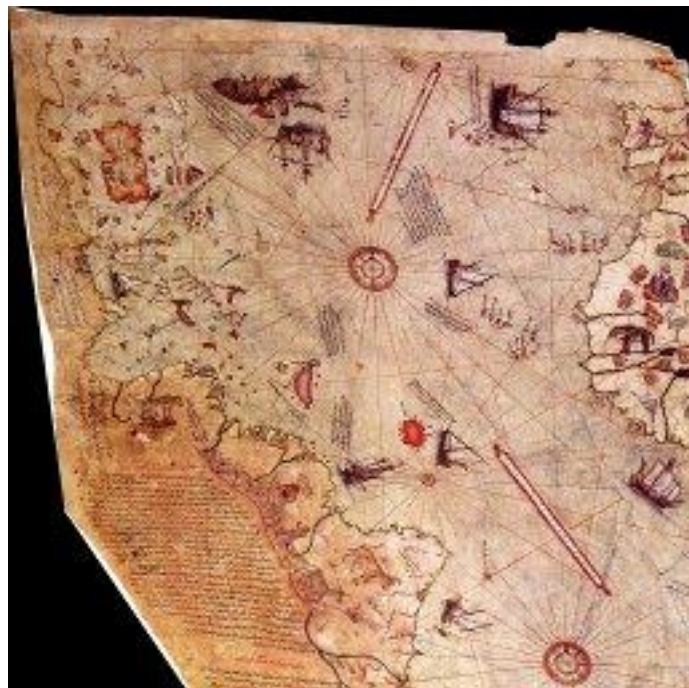


Figure A.18 Ancient Piri Reis Map

APPENDIX B

SOURCE CODE

```
TransformImage : Transforms Image and builds image pyramid hierachy
package com.bilgi.geodb.stream.tile;

import java.awt.image.BufferedImage;
import java.io.BufferedWriter;
import java.io.DataInputStream;
import java.io.DataOutputStream;
import java.io.File;
import java.io.FileInputStream;
import java.io.FileOutputStream;
import java.io.IOException;
import java.io.InputStream;
import java.io.Writer;
import java.util.ArrayList;
import java.util.Hashtable;
import java.util.Iterator;
import java.util.StringTokenizer;

import javax.imageio.ImageIO;
import javax.swing.ImageIcon;
import javax.swing.JOptionPane;

import kdu_jni.KduException;

import com.bilgi.geodb.jp2.Jp2Util;
import com.bilgi.geodb.stream.test.QualityMetrics;
import com.bilgi.geodb.transform.AbstractIntegerLifting;
import com.bilgi.geodb.transform.HaarIntegerLifting;
import com.bilgi.geodb.transform.W2x4;
import com.bilgi.geodb.transform.W4x2;
import com.bilgi.geodb.transform.W4x4;
import com.bilgi.geodb.transform.W5X3Lifting;

public class TransformImage
{
    public String wwCacheBase;
    public static long allSNRDifJPG = 0;
    public static int count = 0;
    public static int streamvsJPEGBetter;
    public static int jp2IsBetter;
    public static int jpegIsBetter;
    public static int streamvsJP2Better;
    public static long allSNRDifJP2;
```

```

AbstractIntegerLifting transformer = new W5X3Lifting();

public TransformImage()
{
}

public TransformImage(String worldWindCacheBase)
{
    this.wwCacheBase = worldWindCacheBase;
}

public TransformImage(AbstractIntegerLifting lifting) {
    this.transformer = lifting;
}

public Hashtable<String, short[][]> transformImage(BufferedImage
input, int level, int minx, int miny, int minPyramidLevel)
{
    int numberOfBands =
input.getTransparency() !=BufferedImage.OPAQUE?4:3;

    int[][] inputData = new int[numberOfBands][input.getWidth() *
input.getHeight()];
    short[][] inputData2 = new short[numberOfBands][input.getWidth()
* input.getHeight()];

    int origWidth = input.getWidth();
    int origHeight = input.getHeight();

    short[][][] sample = new short[numberOfBands][][];

    for (int i = 0; i < numberOfBands; ++i) {
        input.getData().getSamples(0, 0, input.getWidth(),
input.getHeight(), i, inputData[i]);
    }

    for (int i = 0; i < inputData[0].length; ++i) {
        short R = (short)inputData[0][i];
        short G = (short)inputData[1][i];
        short B = (short)inputData[2][i];

        short[] YDD = AbstractIntegerLifting.RGBtoYDD(new short[] { R,
G, B });

        for (int j = 0; j < 3; ++j) {
            inputData2[j][i] = YDD[j];
        }
        if(numberOfBands==4)
            inputData2[3][i] = (short)inputData[3][i];
    }

    Hashtable result = new Hashtable();

```

```

for (int k = level; k > 0; --k) {
    short[][][] bandHighs = new short[numberOfBands][][];
    int numOfParts = 0;
    for (int i = 0; i < numberOfBands; ++i) {
        short[][] temp = transformer.lift2d(inputData2[i]);
        inputData2[i] = temp[0];
        int tmpSize = (int)Math.sqrt(temp[0].length);
        numOfParts = tmpSize / 128;

        short[][] highParts = new short[numOfParts][numOfParts];

        for (int r = 0; r < numOfParts; ++r) {
            for (int c = 0; c < numOfParts; ++c)
                highParts[c][r] = new short[49152];

        }

        for (int coef = 1; coef < 4; ++coef)
            for (int r = 0; r < numOfParts; ++r)
                for (int c = 0; c < numOfParts; ++c)
                    for (int tmpR = 0; tmpR < 128; ++tmpR)
                        System.arraycopy(temp[coef], c * 128 + (r * 128 +
tmpR) * tmpSize, highParts[c][r], (coef - 1) * 16384 + tmpR * 128,
128);

        bandHighs[i] = highParts;
    }

    for (int i = 0; i < numOfParts; ++i)
        for (int j = 0; j < numOfParts; ++j) {
            short[][] tmp = new short[numberOfBands][];
            for (int b = 0; b < numberOfBands; ++b)
                tmp[b] = bandHighs[b][i][(numOfParts - 1 - j)];
            result.put((minPyramidLevel + k) + "_" + ((minx << k) + i)
+ "_" + ((miny << k) + j), tmp);
        }

    }

    short[][] tmp = new short[numberOfBands][];

    for (int i = 0; i < numberOfBands; ++i) {
        tmp[i] = inputData2[i];
    }

    result.put(minPyramidLevel + "_" + minx + "_" + miny, tmp);

    return result;
}

public BufferedImage createBufferedImage(int[][] data, boolean

```

```

isLow)
{
    int dim1 = 128;
    if (isLow)
        dim1 = (int)Math.sqrt(data[0].length);

    int dim2 = data[0].length / dim1;

    int type = data.length
    ==4?BufferedImage.TYPE_INT_ARGB:BufferedImage.TYPE_INT_RGB;

    BufferedImage result = new BufferedImage(dim1, dim2, type);
    for (int j = 0; j < dim2; ++j)
        for (int i = 0; i < dim1; ++i) {
            short[] rgb = AbstractIntegerLifting.YDDtoRGB(new short[] {
(short)data[0][(i + j * dim1)], (short)data[1][(i + j * dim1)],
(short)data[2][(i + j * dim1)] });
            int rgbPack = rgb[0] << 16 | rgb[1] << 8 | rgb[2];
            if(data.length ==4)
                rgbPack = rgbPack | data[3][(i + j * dim1)] << 24;
            result.setRGB(i, j, rgbPack);
        }

    return result;
}

public int[][] inverseTransform(int[][] low, int[][] high, int
row, int col)
{
    int[][] result = new int[low.length][65536];
    int[][] curLow = new int[low.length][16384];

    int tcol = 1 - col;
    for (int i = 0; i < low.length; ++i) {
        for (int r = 0; r < 128; ++r) {
            try{
                System.arraycopy(low[i], 128 * row + (r + 128 * tcol) * 256,
curLow[i], r * 128, 128);
            }
            catch (Exception e) {
//                e.printStackTrace();
            }
        }
    }

    for (int i = 0; i < low.length; ++i)
    {
        int[][] coefs = new int[4][16384];
        coefs[0] = curLow[i];

        for (int j = 0; j < 3; ++j) {
            System.arraycopy(high[i], j * 128 * 128, coefs[(j + 1)], 0,
16384);

```

```

    }

    result[i] = transformer.unlift2d(coefs);

    }

    return result;
}

public int[] getTileStreamSamples(InputStream inStream)
    throws IOException, KduException
{
    DataInputStream stream2 = new DataInputStream(inStream);
    int rlev = stream2.readInt();
    int rx = stream2.readInt();
    int ry = stream2.readInt();
    int layerNameLength = stream2.readInt();
    String lyrName = "";
    for (int i = 0; i < layerNameLength; ++i)
        lyrName = lyrName + stream2.readChar();
    int[] result = new int[65536];
    BufferedImage bim = getTileImage(rlev, rx, ry, lyrName);
    bim.getRGB(0, 0, 256, 256, result, 0, 256);
    return result;
}

public BufferedImage getTileImage(int level, int x, int y, String
layerName)
    throws IOException
{
    int waveletLevel = level % 4;

    int baseX = x >> waveletLevel;
    int baseY = y >> waveletLevel;

    TileIndex index = new TileIndex(level - waveletLevel, baseX,
baseY);
    FileInputStream streamBase = new FileInputStream(new File(
//
        wwCacheBase+layerName+File.separatorChar+index.getGeobsCachePa
th()

        "/data/imigiTest/"+index.level+"_"+index.xIndex+"_"+index.yInd
ex+".jp2"

        ));

    int[][] low = getTileCoefs(streamBase);

    streamBase.close();

    for (int i = waveletLevel - 1; i >= 0; --i) {
        int highLevel = level - i;
        int highX = x >> i;
        int highY = y >> i;

```

```

        TileIndex tindex = new TileIndex(highLevel, highX, highY);
        FileInputStream stream = new FileInputStream(new File(
//
        wwCacheBase+layerName+File.separatorChar+tindex.getGeobsCacheP
        ath()

        "/data/imigiTest/"+tindex.level+"_"+tindex.xIndex+"_"+tindex.y
        Index+".jp2"

                ));

        int[][] high = getTileCoefs(stream);
        stream.close();

        int col = highX % 2;
        int row = highY % 2;

        low = inverseTransform(low, high, col, row);
    }

    return createBufferedImage(low, true);
}

public int[][] getTileCoefs(InputStream stream)
{
    int[][] result;
    try
    {
        DataInputStream stream2 = new DataInputStream(stream);

        int rlev = stream2.readInt();
        int rx = stream2.readInt();
        int ry = stream2.readInt();
        int layerNameLength = stream2.readInt();
        String lyrName = "";
        for (int i = 0; i < layerNameLength; ++i)
            lyrName = lyrName + stream2.readChar();

        result = Jp2Util.decodeShortBands(stream);
    } catch (Exception e) {
        return null;
    }

    return result;
}
}

```

TileIndex : Tile index structure for progressive image tiles

```
package com.bilgi.geodb.stream.tile;

import java.io.File;
import java.util.ArrayList;

public class TileIndex {

    public int level;
    public int xIndex;
    public int yIndex;

    public static final int transformLevel = 4;

    public TileIndex(int level, int xIndex, int yIndex){
        this.level = level;
        this.xIndex = xIndex;
        this.yIndex = yIndex;
    }

    public String getGeobsCachePath(){
        return
        ""+level+File.separatorChar+yIndex+File.separatorChar+yIndex+" "+xIndex+
        ".jp2";
    }

    public ArrayList<TileIndex> getRequiredTiles(){
        ArrayList<TileIndex> result = new
        ArrayList<TileIndex>();
        int waveletLevel = level % transformLevel;

        int baseX = xIndex>>waveletLevel;
        int baseY = yIndex>>waveletLevel;

        result.add(new TileIndex(level - waveletLevel,baseX
        ,baseY));

        for(int i=waveletLevel-1;i>=0;i--){
            int highLevel = level-i;
            int highX = xIndex>>i;
            int highY = yIndex>>i;
            result.add(new TileIndex(highLevel, highX,
            highY));
        }

        return result;
    }
}
```

AbstractIntegerLifting : Integer Lifting Kernels extends this class

```
package com.bilgi.geodb.transform;

public abstract class AbstractIntegerLifting
{
    public static int EVEN = 0;
    public static int ODD = 1;
    public static int AVERAGE = 0;
    public static int DIFFERENCE = 1;
    public static int LL = 0;
    public static int LH = 1;
    public static int HL = 2;
    public static int HH = 3;

    protected short[][] split(short[] data)
    {
        short[][] result = new short[2][data.length / 2];

        for (int i = 0; i < data.length / 2; ++i) {
            result[EVEN][i] = data[i * 2];
            result[ODD][i] = data[i * 2 + 1];
        }

        return result;
    }

    protected short[] merge(short[] even, short[] odd) {
        short[] result = new short[even.length * 2];

        for (int i = 0; i < even.length; ++i) {
            result[(i * 2)] = even[i];
            result[(i * 2 + 1)] = odd[i];
        }

        return result;
    }

    protected void add(short[] data1, short[] data2) {
        for (int i = 0; i < data1.length; ++i) {
            int tmp10_9 = i;
            short[] tmp10_8 = data1; tmp10_8[tmp10_9] =
(short) (tmp10_8[tmp10_9] + data2[i]); }
    }

    protected void subtract(short[] data1, short[] data2) {
        for (int i = 0; i < data1.length; ++i) {
            int tmp10_9 = i;
            short[] tmp10_8 = data1;
            tmp10_8[tmp10_9] = (short) (tmp10_8[tmp10_9] - data2[i]);
        }
    }

    protected abstract short[] predict(short[] paramArrayOfShort);
    protected abstract short[] update(short[] paramArrayOfShort);
}
```

```

public short[][] lift(short[] line) {
    short[][] splitted = split(line);

    subtract(splitted[ODD], predict(splitted[EVEN]));
    add(splitted[EVEN], update(splitted[ODD]));

    return splitted;
}

public short[] unlift(short[] difference, short[] average)
{
    subtract(average, update(difference));
    add(difference, predict(average));

    return merge(average, difference);
}

public short[][] lift2d(short[] LL)
{
    short[][] result = new short[4][];

    int width = (int)Math.sqrt(LL.length);

    short[] low = new short[width * width / 2];
    short[] high = new short[width * width / 2];

    short[] tempLL = new short[(int)Math.sqrt(LL.length)];

    for (int i = 0; i < width; ++i) {
        System.arraycopy(LL, i * width, tempLL, 0, width);

        short[][] temp = lift(tempLL);

        System.arraycopy(temp[AVERAGE], 0, low, i * width / 2, width /
2);
        System.arraycopy(temp[DIFFERENCE], 0, high, i * width / 2,
width / 2);
    }

    short[] lowlow = new short[width * width / 4];
    short[] lowhigh = new short[width * width / 4];
    short[] highlow = new short[width * width / 4];
    short[] highhigh = new short[width * width / 4];

    for (int i = 0; i < width / 2; ++i)
    {
        short[] tempLow = new short[width];
        short[] tempHigh = new short[width];
        for (int j = 0; j < width; ++j) {
            tempLow[j] = low[(i + j * width / 2)];
            tempHigh[j] = high[(i + j * width / 2)];
        }

        short[][] temp = lift(tempLow);

```

```

short[][] temp2 = lift(tempHigh);

for(int j=0;j<width/2;j++){

    lowlow[i+j*width/2] = temp[AVERAGE][j];
    lowhigh[i+j*width/2] = temp[DIFFERENCE][j];

    highlow[i+j*width/2] = temp2[AVERAGE][j];
    highhigh[i+j*width/2] = temp2[DIFFERENCE][j];
}

}

result[AbstractIntegerLifting.LL] = lowlow;
result[LH] = lowhigh;
result[HL] = highlow;
result[HH] = highhigh;

return result;
}

public short[] unlift2d(short[][] coeff)
{
short[] result = new short[coeff[LL].length * 4];

short preWith = (short) (int)Math.sqrt(coeff[LL].length);

short[][] low = new short[preWith * 2][preWith];
short[][] high = new short[preWith * 2][preWith];

for (int i = 0; i < preWith; ++i) {
short[] tempL = new short[preWith];
short[] tempH = new short[preWith];

for(int j=0;j<preWith;j++){
tempL[j]= coeff[LL][i+j*preWith];
tempH[j]= coeff[LH][i+j*preWith];
}

short[] tempLow = unlift(tempH, tempL);

for(int j=0;j<preWith;j++){
tempL[j]= coeff[HL][i+j*preWith];
tempH[j]= coeff[HH][i+j*preWith];
}

short[] tempHigh = unlift(tempH, tempL);

for (int j = 0; j < preWith * 2; ++j) {
low[j][i] = tempLow[j];
high[j][i] = tempHigh[j];
}
}
for (int i = 0; i < preWith * 2; ++i) {

```

```

        short[] temp = unlift(high[i], low[i]);
        System.arraycopy(temp, 0, result, preWith * i * 2, preWith *
2);
    }

    return result;
}

public short[][] WT2D(short[] source, int level)
{
    short[][] result = new short[1 + level * 3][];

    short[] LL = source;

    for (int i = level; i > 0; --i) {
        short[][] temp = lift2d(LL);

        for (int j = 2; j >= 0; --j)
            result[(i * 3 - j)] = temp[(j + 1)];

        LL = temp[0];
    }

    result[0] = LL;
    return result;
}

public short[] IWT2D(short[][] coefStack, int level) {
    short[] result = new short[coefStack[0].length << level * 2];

    short[][] temp = new short[4][];

    temp[LL] = coefStack[0];

    for (int i = 1; i <= level; ++i) {
        for (int j = 3; j > 0; --j)
            temp[j] = coefStack[(i * 3 - j + 1)];
        temp[0] = unlift2d(temp);
    }
    result = temp[0];
    return result;
}

////////////////////////////////////
////////////////////////////////////
protected int[][] split(int[] data)
{
    int[][] result = new int[2][data.length / 2];

    for (int i = 0; i < data.length / 2; ++i) {
        result[EVEN][i] = data[(i * 2)];
        result[ODD][i] = data[(i * 2 + 1)];
    }
}

```

```

    return result;
}

protected int[] merge(int[] even, int[] odd) {
    int[] result = new int[even.length * 2];

    for (int i = 0; i < even.length; ++i) {
        result[(i * 2)] = even[i];
        result[(i * 2 + 1)] = odd[i];
    }

    return result;
}

protected void add(int[] data1, int[] data2) {
    for (int i = 0; i < data1.length; ++i) {
        int tmp10_9 = i;
        int[] tmp10_8 = data1; tmp10_8[tmp10_9] =
(int) (tmp10_8[tmp10_9] + data2[i]); }
    }

protected void subtract(int[] data1, int[] data2) {
    for (int i = 0; i < data1.length; ++i) {
        int tmp10_9 = i;
        int[] tmp10_8 = data1; tmp10_8[tmp10_9] =
(int) (tmp10_8[tmp10_9] - data2[i]);
    }
}

protected abstract int[] predict(int[] paramArrayOfint);

protected abstract int[] update(int[] paramArrayOfint);

public int[][] lift(int[] line) {
    int[][] splitted = split(line);

    subtract(splitted[ODD], predict(splitted[EVEN]));
    add(splitted[EVEN], update(splitted[ODD]));

    return splitted;
}

public int[] unlift(int[] difference, int[] average)
{
    subtract(average, update(difference));
    add(difference, predict(average));

    return merge(average, difference);
}

public int[][] lift2d(int[] LL)
{
    int[][] result = new int[4][];

    int width = (int) Math.sqrt(LL.length);

```

```

int[] low = new int[width * width / 2];
int[] high = new int[width * width / 2];

int[] tempLL = new int[(int)Math.sqrt(LL.length)];

for (int i = 0; i < width; ++i) {
    System.arraycopy(LL, i * width, tempLL, 0, width);

    int[][] temp = lift(tempLL);

    System.arraycopy(temp[AVERAGE], 0, low, i * width / 2, width /
2);
    System.arraycopy(temp[DIFFERENCE], 0, high, i * width / 2,
width / 2);
}

int[] lowlow = new int[width * width / 4];
int[] lowhigh = new int[width * width / 4];
int[] highlow = new int[width * width / 4];
int[] highhigh = new int[width * width / 4];

for (int i = 0; i < width / 2; ++i)
{
    int[] tempLow = new int[width];
    int[] tempHigh = new int[width];
    for (int j = 0; j < width; ++j) {
        tempLow[j] = low[(i + j * width / 2)];
        tempHigh[j] = high[(i + j * width / 2)];
    }

    int[][] temp = lift(tempLow);
    int[][] temp2 = lift(tempHigh);

    for(int j=0;j<width/2;j++){

        lowlow[i+j*width/2] = temp[AVERAGE][j];
        lowhigh[i+j*width/2] = temp[DIFFERENCE][j];

        highlow[i+j*width/2] = temp2[AVERAGE][j];
        highhigh[i+j*width/2] = temp2[DIFFERENCE][j];
    }

}

result[AbstractIntegerLifting.LL] = lowlow;
result[LH] = lowhigh;
result[HL] = highlow;
result[HH] = highhigh;

return result;
}

public int[] unlift2d(int[][] coeff)
{

```

```

int[] result = new int[coeff[LL].length * 4];

int preWith = (int) (int) Math.sqrt(coeff[LL].length);

int[][] low = new int[preWith * 2][preWith];
int[][] high = new int[preWith * 2][preWith];

for (int i = 0; i < preWith; ++i) {
    int[] tempL = new int[preWith];
    int[] tempH = new int[preWith];

    for(int j=0;j<preWith;j++){
        tempL[j]= coeff[LL][i+j*preWith];
        tempH[j]= coeff[LH][i+j*preWith];
    }

    int[] tempLow = unlift(tempH, tempL);

    for(int j=0;j<preWith;j++){
        tempL[j]= coeff[HL][i+j*preWith];
        tempH[j]= coeff[HH][i+j*preWith];
    }

    int[] tempHigh = unlift(tempH, tempL);

    for (int j = 0; j < preWith * 2; ++j) {
        low[j][i] = tempLow[j];
        high[j][i] = tempHigh[j];
    }
}
for (int i = 0; i < preWith * 2; ++i) {
    int[] temp = unlift(high[i], low[i]);
    System.arraycopy(temp, 0, result, preWith * i * 2, preWith * 2);
}

return result;
}

public int[][] WT2D(int[] source, int level)
{
    int[][] result = new int[1 + level * 3][];

    int[] LL = source;

    for (int i = level; i > 0; --i) {
        int[][] temp = lift2d(LL);

        for (int j = 2; j >= 0; --j)
            result[(i * 3 - j)] = temp[(j + 1)];

        LL = temp[0];
    }

    result[0] = LL;
}

```

```

    return result;
}

public int[] IWT2D(int[][] coefStack, int level) {
    int[] result = new int[coefStack[0].length << level * 2];

    int[][] temp = new int[4][];

    temp[LL] = coefStack[0];
    for (int i = 1; i <= level; ++i) {
        for (int j = 3; j > 0; --j)
            temp[j] = coefStack[(i * 3 - j + 1)];
        temp[0] = unlift2d(temp);
    }
    result = temp[0];
    return result;
}

public static short[] RGBtoYDD(short[] rgb) {
    short[] result = new short[3];

    short r = rgb[0];
    short g = rgb[1];
    short b = rgb[2];

    short y = g;
    short db = (short)(b - g);
    short dr = (short)(r - g);

    result[0] = y;
    result[1] = db;
    result[2] = dr;

    return result;
}

public static short[] YDDtoRGB(short[] YDD) {
    short[] result = new short[3];

    short y = YDD[0];
    short db = YDD[1];
    short dr = YDD[2];

    short g = y;
    short r = (short)(y + dr);
    short b = (short)(y + db);

    result[0] = (short)Math.min(Math.max(0, r), 255);
    result[1] = (short)Math.min(Math.max(0, g), 255);
    result[2] = (short)Math.min(Math.max(0, b), 255);

    return result;
}
}

```

HaarIntegerLifting : Haar lifting implementation of AbstractIntegerLifting

```
package com.bilgi.geodb.transform;
public class HaarIntegerLifting extends AbstractIntegerLifting
{
    protected short[] predict(short[] data)
    {
        return data;
    }

    protected short[] update(short[] data)
    {
        short[] result = new short[data.length];
        for (int i = 0; i < data.length; ++i) {
            result[i] = (short) (data[i] / 2);
        }

        return result;
    }

    @Override
    protected int[] predict(int[] data) {
        return data;
    }

    @Override
    protected int[] update(int[] data) {
        int[] result = new int[data.length];
        for (int i = 0; i < data.length; ++i) {
            result[i] = (short) (data[i] / 2);
        }

        return result;
    }
}
```

W5x3 : W5x3 lifting implementation of AbstractIntegerLifting

```
package com.bilgi.geodb.transform;

public class W5X3Lifting extends AbstractIntegerLifting{

    @Override
    protected short[] predict(short[] data) {

        short []result = new short[data.length];

        result[data.length-1]=data[data.length-1] ;

        for(int i=0;i<data.length-1;i++){
            result[i]= (short) (((data[i+1])+(data[i]))/2.0f);
        }

        return result;
    }
}
```

```

    }

    @Override
    protected short[] update(short[] data) {

        short []result = new short[data.length];

        result[0]= (short)((data[0])/2) ;

        for(int i=1;i<data.length;i++){
            result[i]= (short)(((data[i-1])+(data[i]))/4.0f);
        }

        return result;
    }

    @Override
    protected int[] predict(int[] data) {
        int []result = new int[data.length];

        result[data.length-1]=data[data.length-1] ;

        for(int i=0;i<data.length-1;i++){
            result[i]= (short)(((data[i+1])+(data[i]))/2.0f);
        }

        return result;
    }

    @Override
    protected int[] update(int[] data) {
        int []result = new int[data.length];

        result[0]= (short)((data[0])/2) ;

        for(int i=1;i<data.length;i++){
            result[i]= (short)(((data[i-1])+(data[i]))/4.0f);
        }

        return result;
    }
}

```

W2x4 : WI2x4 interpolating lifting implementation of AbstractIntegerLifting

```
package com.bilgi.geodb.transform;

public class W2x4 extends AbstractIntegerLifting{

    @Override
    protected short[] predict(short[] data) {

        short []result = new short[data.length];

        result[data.length-1]=data[data.length-1] ;

        for(int i=0;i<data.length-1;i++){
            result[i]= (short) (((data[i+1]))+(data[i]))/2.0f);
        }

        return result;
    }

    @Override
    protected int[] predict(int[] data) {
        int []result = new int[data.length];

        result[data.length-1]=data[data.length-1] ;

        for(int i=0;i<data.length-1;i++){
            result[i]= (short) (((data[i+1]))+(data[i]))/2.0f);
        }

        return result;
    }

    @Override
    protected short[] update(short[] data) {
        short[] result = new short[data.length];

        result[0]= (short) (19/64*(data[0]+data[0]) -
3/64*(data[0]+data[1]));
        result[1]= (short) (19/64*(data[0]+data[1]) -
3/64*(data[0]+data[2]));
        result[data.length-1]= (short) (19/64*(data[data.length-
2]+data[data.length-1])
- 3/64*(data[data.length-
3]+data[data.length-1]));

        for(int i=2;i<data.length-1;i++){
            result[i]= (short) (19/64*(data[i-1]+data[i]) -
3/64*(data[i-2]+data[i+1]));
        }

        return result;
    }

    @Override
```

```

protected int[] update(int[] data) {
    int[] result = new int[data.length];

    result[0]= (short) (19/64*(data[0]+data[0]) -
3/64*(data[0]+data[1]));
    result[1]= (short) (19/64*(data[0]+data[1]) -
3/64*(data[0]+data[2]));
    result[data.length-1]= (short) (19/64*(data[data.length-
2]+data[data.length-1])
- 3/64*(data[data.length-
3]+data[data.length-1]));

    for(int i=2;i<data.length-1;i++){
        result[i]= (short) (19/64*(data[i-1]+data[i]) -
3/64*(data[i-2]+data[i+1]));
    }

    return result;
}
}

```

W4x2 : W14x2 interpolating lifting implementation of AbstractIntegerLifting

```

package com.bilgi.geodb.transform;

public class W4x2 extends AbstractIntegerLifting{

    @Override
    protected short[] predict(short[] data) {
        short []result = new short[data.length];

        result[0]= (short) (9/16*(data[0]+data[1]) -
1/16*(data[0]+data[2]));
        result[data.length-1] = (short) (9/16*(data[data.length-
1]+data[data.length-1])
- 1/16*(data[data.length-
2]+data[data.length-1]));

        result[data.length-2] = (short) (9/16*(data[data.length-
2]+data[data.length-1])
- 1/16*(data[data.length-
3]+data[data.length-1]));

        for(int i=1;i<data.length-2;i++){
            result[i]= (short) (9/16*(data[i]+data[i+1]) -
1/16*(data[i-1]+data[i+2]));
        }

        return result;
    }
}

```

```

    @Override
    protected int[] predict(int[] data) {
        int []result = new int[data.length];

        result[0]= (short) (9/16*(data[0]+data[1]) -
1/16*(data[0]+data[2]));
        result[data.length-1] = (short) (9/16*(data[data.length-
1]+data[data.length-1])
            - 1/16*(data[data.length-
2]+data[data.length-1]));

        result[data.length-2] = (short) (9/16*(data[data.length-
2]+data[data.length-1])
            - 1/16*(data[data.length-
3]+data[data.length-1]));

        for(int i=1;i<data.length-2;i++){
            result[i]= (short) (9/16*(data[i]+data[i+1]) -
1/16*(data[i-1]+data[i+2]));
        }

        return result;
    }

    @Override
    protected short[] update(short[] data) {
        short []result = new short[data.length];

        result[0]= (short) (data[0]/2) ;

        for(int i=1;i<data.length;i++){
            result[i]= (short) (((data[i-1])+(data[i]))/4.0f);
        }

        return result;
    }

    @Override
    protected int[] update(int[] data) {
        int []result = new int[data.length];

        result[0]= (short) (data[0]/2) ;

        for(int i=1;i<data.length;i++){
            result[i]= (short) (((data[i-1])+(data[i]))/4.0f);
        }

        return result;
    }
}

```

W4x4 : WI4x4 interpolating lifting implementation of AbstractIntegerLifting

```

package com.bilgi.geodb.transform;

public class W4x4 extends AbstractIntegerLifting{

    @Override
    protected short[] predict(short[] data) {
        short[] result = new short[data.length];

        result[0]= (short) (19/64*(data[0]+data[0]) -
3/64*(data[0]+data[1]));
        result[1]= (short) (19/64*(data[0]+data[1]) -
3/64*(data[0]+data[2]));
        result[data.length-1]= (short) (19/64*(data[data.length-
2]+data[data.length-1])
        - 3/64*(data[data.length-
3]+data[data.length-1]));

        for(int i=2;i<data.length-1;i++){
            result[i]= (short) (19/64*(data[i-1]+data[i]) -
3/64*(data[i-2]+data[i+1]));
        }

        return result;
    }

    @Override
    protected int[] predict(int[] data) {
        int[] result = new int[data.length];

        result[0]= (short) (19/64*(data[0]+data[0]) -
3/64*(data[0]+data[1]));
        result[1]= (short) (19/64*(data[0]+data[1]) -
3/64*(data[0]+data[2]));
        result[data.length-1]= (short) (19/64*(data[data.length-
2]+data[data.length-1])
        - 3/64*(data[data.length-
3]+data[data.length-1]));

        for(int i=2;i<data.length-1;i++){
            result[i]= (short) (19/64*(data[i-1]+data[i]) -
3/64*(data[i-2]+data[i+1]));
        }

        return result;
    }

    @Override
    protected short[] update(short[] data) {
        short[] result = new short[data.length];

        result[0]= (short) (19/64*(data[0]+data[0]) -
3/64*(data[0]+data[1]));
        result[1]= (short) (19/64*(data[0]+data[1]) -

```

```

3/64*(data[0]+data[2]));
        result[data.length-1]= (short) (19/64*(data[data.length-
2]+data[data.length-1])
        - 3/64*(data[data.length-
3]+data[data.length-1]));

        for(int i=2;i<data.length-1;i++){
            result[i]= (short) (19/64*(data[i-1]+data[i]) -
3/64*(data[i-2]+data[i+1]));
        }

        return result;
    }

    @Override
    protected int[] update(int[] data) {
        int[] result = new int[data.length];

        result[0]= (short) (19/64*(data[0]+data[0]) -
3/64*(data[0]+data[1]));
        result[1]= (short) (19/64*(data[0]+data[1]) -
3/64*(data[0]+data[2]));
        result[data.length-1]= (short) (19/64*(data[data.length-
2]+data[data.length-1])
        - 3/64*(data[data.length-
3]+data[data.length-1]));

        for(int i=2;i<data.length-1;i++){
            result[i]= (short) (19/64*(data[i-1]+data[i]) -
3/64*(data[i-2]+data[i+1]));
        }

        return result;
    }
}

```